Cell-specialized chloroplast signaling orchestrates photosynthetic and extracellular reactive oxygen species for stress responses

Estee E. Tee[1,5], Stephen J. Fairweather[1], Hanh M. Vo[1,6], Chenchen Zhao[2,7], Andrew Breakspear[3], Sachie Kimura[4,8], Melanie Carmody[4,9], Michael Wrzaczek[4,10,11], Stefan Bröer[1], Christine Faulkner[3], Jaakko Kangasjärvi[4], Zhong-Hua Chen[2], Barry J. Pogson[1*], Kai Xun Chan[1*]

[1]Research School of Biology, Australian National University, 2601 Canberra, Australia

[2]School of Science, Western Sydney University, 2753 Sydney, Australia

[3]Cell and Developmental Biology, John Innes Centre, NR4 7UH Norwich, United Kingdom

[4]Organismal and Evolutionary Biology, Viiki Plant Science Centre, University of Helsinki, 00014 Helsinki, Finland

[5]Present address: Cell and Developmental Biology, John Innes Centre, NR4 7UH Norwich, United Kingdom

[6]Present address: School of Natural Sciences, University of Tasmania, 7001 Hobart, Australia

[7]Present address: Tasmanian Institute of Agriculture, University of Tasmania, 7250 Launceston, Australia

[8]Present address: NAPIGEN, Inc., 19803 Delaware, United States of America

[9]Present address: Synthetic Biology Future Science Platform, Commonwealth Scientific and Industrial Research Organisation, 2601 Canberra, Australia

[10]Present address: Institute of Plant Molecular Biology, Czech Academy of Sciences, 370 05 České Budějovice, Czech Republic

[11]Present address: University of South Bohemia, Faculty of Science, Department of Experimental Plant Biology, 370 05 České Budějovice, Czech Republic

[*] **Authors for Correspondence:** kai.chan@anu.edu.au and barry.pogson@anu.edu.au

Author Contributions: E.E.T., S.J.F., S.K., M.C., M.W., S.B., C.F., J.K., Z.H.C., B.J.P. and K.X.C. designed research; E.E.T., S.J.F., H.M.V., C.Z., A.B. and K.X.C. performed research; E.E.T., S.J.F., H.M.V. analyzed data; E.E.T., B.J.P., and K.X.C. wrote the paper with contribution from all authors.

Competing Interest Statement: No competing interests to declare.

Classification: Plant Biology

Keywords: Chloroplast, ROS, retrograde signaling, stomata, calcium dependent protein kinase

This PDF file includes:

Main Text

Figures 1 to 5

Abstract

Cellular responses to abiotic stress involve multiple signals including secondary messengers such as reactive oxygen species (ROS) and Ca^{2+}, phytohormones such as abscisic acid (ABA) and chloroplast-to-nucleus retrograde signals such as 3'-phosphoadenosine 5'-phosphate (PAP). Mechanism(s) by which these messengers, produced in different subcellular compartments, intersect for cell regulation remain enigmatic. Previously we showed that the chloroplast retrograde signal PAP, similar to ABA, induces an increase in ROS levels in guard cells (Pornsiriwong *et al*, 2017). Here we demonstrate a mechanistic link enabling ABA and PAP to coordinate both chloroplast and plasma membrane ROS production. In whole leaves, PAP alters various ROS-related processes including plasmodesmal permeability as well as responses to ozone and the bacterial elicitor flg22, but mainly initiates processes that quench ROS during oxidative stress. Conversely, we show in guard cells, both PAP and ABA induce an increase in ROS levels in both chloroplasts via photosynthetic electron transport, and the apoplast via the RESPIRATORY BURST OXIDASE HOMOLOG (RBOH). Both subcellular ROS sources were necessary for ABA- and PAP-mediated stomatal closure. However, PAP signaling diverges from ABA by activating RBOHD, instead of RBOHF, for apoplastic ROS mediated stomatal closure. We identified three calcium-dependent protein kinases (CPKs) as the post-translational activators of RBOHD-mediated ROS production. CPK13, CPK32, and CPK34 were transcriptionally induced by PAP and concurrently activate RBOHD and the slow anion channel SLAC1 by phosphorylating two Serine (S) residues, including S120 which is also targeted by the core ABA signaling kinase OPEN STOMATA 1 (OST1). Consequently, overexpression of the PAP-induced CPKs rescues stomatal closure in *ost1.* Our data identify stomatal chloroplasts, to be nodes in the multifaceted cellular stress response networks as they are both sources and mediators of ROS and retrograde signals such PAP. Thus, chloroplasts are not just mediators of photosynthesis in response to, for example, excess light, but can serve as critical nodes in the multifaceted cellular stress response networks in specialized cells via retrograde signals, providing support to the concept of sensory plastids.

65 **Significance Statement**

66 The chloroplast is an environmental sensor for stresses such as excess light and drought via the
67 activation of photosynthetic-mediated retrograde signals. However, how does it function in
68 specialized cells for which carbon fixation is secondary? Here we show the chloroplast is an
69 important node to coordinate multiple plant signaling pathways in response to stresses such as
70 drought. The chloroplast retrograde signal 3'-phosphoadenosine 5'-phosphate (PAP) plays multiple
71 roles in reactive oxygen species (ROS) signaling and homeostasis. While PAP suppresses ROS
72 in photosynthetic tissue, PAP instead induces guard cell ROS in chloroplasts and extracellular
73 space to induce stomatal closure. We decipher how PAP-induced proteins activate both
74 extracellular ROS production and anion channels for stomatal closure, thus providing a mechanism
75 by which chloroplasts provide a strategic complement to canonical hormonal pathways in regulating
76 plant physiological responses in specialized cells.

77 **Introduction**

78

79 Plant responses to abiotic and biotic stresses involve a suite of coordinated cellular signaling
80 cascades. These involve multiple messenger molecules including reactive oxygen species (ROS),
81 calcium ions (Ca^{2+}), phytohormones such as abscisic acid (ABA), and retrograde signals, defined
82 as signals from an organelle (i.e., the chloroplast or mitochondria) that regulate nuclear gene
83 expression (Chan et al., 2016b; Cutler et al., 2010; Waszczak et al., 2018). While each of the
84 aforementioned messengers have been extensively studied, their spatio-temporal intersections
85 remain enigmatic. For example, both apoplastic ROS and organelle-to-nucleus retrograde signals
86 occur concurrently, yet it is unclear how these two classes of signals interact and are coordinated
87 in specialized cells. This is relevant to the proposition that plants have specialized plastids for
88 sensing and signaling (Mackenzie and Mullineaux, 2022).

89

90 ROS are crucial signaling molecules produced in diverse subcellular compartments including
91 chloroplasts and the apoplast. Several types of ROS exist in plant cells and distinct ROS types play
92 different signaling roles (Chan et al., 2016b; Cutler et al., 2010; Waszczak et al., 2018), but herein
93 we refer to chloroplast and apoplast "ROS" as an encompassing term for three ROS types formed
94 via similar mechanisms at these subcellular locations: superoxide (O_2^-), its dismutation product
95 hydrogen peroxide (H_2O_2), and hydroxyl radical ($OH\cdot$); with H_2O_2 being the most stable (Waszczak
96 et al., 2018). ROS generated from photosystem I (PSI) in chloroplasts participates in chloroplast-
97 to-nucleus retrograde signaling, both by triggering production of retrograde signals via H_2O_2-
98 responsive redox regulation (Chan et al., 2016a) and by itself acting as a retrograde signal
99 (Exposito-Rodriguez et al., 2017). Silencing the chloroplastic H_2O_2 scavenging enzyme, thylakoid
100 membrane-bound ascorbate peroxidase (tAPX), increased chloroplastic H_2O_2 leading to the up-
101 regulation of multiple stress-associated genes, including pathogen-responsive genes in
102 photosynthetic tissues (Maruta et al., 2012). High light stress increases H_2O_2 production in leaf
103 chloroplasts; the chloroplasts in close physical association with the nucleus can transfer their H_2O_2

104 into the nucleus, potentially representing a direct means for H_2O_2 to act as a retrograde signal to
105 induce nuclear gene expression (Exposito-Rodriguez et al., 2017). However, the nuclear targets of
106 chloroplastic-sourced H_2O_2 are still unknown.
107
108 In contrast to chloroplast PSI ROS, apoplastic superoxide and H_2O_2 are well known to act as
109 secondary messengers in dynamic signaling cascades. One such well characterized pathway that
110 utilizes apoplastic and cellular ROS as a secondary messenger is abscisic acid (ABA)-mediated
111 stomatal closure. In response to an accumulation of ABA under stress conditions such as drought,
112 a simplified guard cell process occurs as follows: ABA forms a complex with PYRABACTIN
113 RESISTANCE 1/PYR1-LIKE/REGULATORY COMPONENTS OF ABA RECEPTORS, with
114 ABSCISIC ACID-INSENSITIVE 1 (ABI1) PP2C phosphatase then binding to the complex (Ma et
115 al., 2009; Park et al., 2009). This removes the inhibition of SUCROSE NON-FERMENTING-1
116 RELATED PROTEIN KINASE (SnRK) 2.6 (SnRK 2.6)/SRK2E/OPEN STOMATA 1 (OST1), which
117 can auto-phosphorylate (Belin et al., 2006; Yoshida et al., 2006). OST1 interacts with
118 RESPIRATORY BURST OXIDASE HOMOLOG F (RBOHF) and RBOHD, leading to RBOH-
119 mediated ROS (superoxide and H_2O_2) production (Acharya et al., 2013; Sirichandra et al., 2009).
120 OST1 also directly regulates the activity of multiple ion channels by phosphorylation, including
121 activation of SLOW ANION CHANNEL 1 (SLAC1) and rapid type anion channel ALMT12 (Acharya
122 et al., 2013; Geiger et al., 2009; Imes et al., 2013), and inhibiting inward rectifying POTASSIUM
123 CHANNEL (KAT1) (Sato et al., 2009). While OST1 has the capacity to directly act on the channels,
124 both ROS and cytosolic Ca^{2+} are required for stomatal closure with H_2O_2 activating Ca^{2+} channels
125 to induce the influx of Ca^{2+} and release of Ca^{2+} from vacuoles and other organelles to the cytosol
126 (Pei et al., 2000; Wang et al., 2013; Wu et al., 2020).
127
128 ROS production via RBOHs is regulated by a suite of different kinases at the whole leaf, tissue,
129 cellular and organellar levels. The Ca^{2+} sensor CALCINEURIN B-LIKE proteins (CBL1; CBL9)
130 interact with CBL-INTERACTING PROTEIN KINASE (CIPK11; CIPK26) to activate RBOHF

131 (Drerup et al., 2013). In contrast, RBOHD is the primary apoplastic ROS generator in response to
132 biotic stimuli and mechanical wounding (Morales et al., 2016; Torres et al., 2002). Regulators of
133 RBOHD activity include several immunity-associated protein kinases (Lee et al., 2020; Li et al.,
134 2014; Zhang et al., 2018), and calcium protein kinases (CPKs). CPK1, CPK2, CPK4, CPK5, CPK6
135 and CPK11 can activate both RBOHD and RBOHF in an immunocomplex kinase assay (Gao et
136 al., 2013), and at least for CPK5, a direct interaction and activation of RBOHD has been confirmed
137 (Dubiella et al., 2013). In guard cells, OST1 activating RBOHF is thought to be the primary pathway
138 for apoplastic ROS production (Sirichandra et al., 2009; Wu et al., 2020). However, the links
139 between ROS production and CPKs as well as the interaction with retrograde signals and the
140 production of apoplastic ROS in guard cells remain elusive, if not illogical from a spatial context.
141
142 The aforementioned leaf chloroplast PSI ROS can trigger other chloroplast-to-nucleus retrograde
143 signaling pathways such as methylerythritol cyclodiphosphate (MEcPP) and SAL1-PAP
144 (3'phosphoadenosine 5'phosphate), the latter of which functions in drought and high light stress
145 (Gonzalo M Estavillo et al., 2011; Xiao et al., 2012). These abiotic stresses promote chloroplast
146 PSI ROS and redox poise which inhibit plastidial SAL1 activity (Chan et al., 2016a), thus allowing
147 accumulation of its catabolic substrate PAP in the cell. In the nucleus, PAP inhibits 5' to 3'
148 exoribonucleases to alter RNA polymerase II function. This leads to read through accumulation of
149 downstream genes in tandem repeats, resulting in accumulation of stress-responsive transcripts
150 including H_2O_2 scavengers (Crisp et al., 2018, 2017). Consequently, *sal1* mutants with
151 constitutively over-accumulated PAP show lower foliar ROS levels, particularly in the vascular
152 bundle (Estavillo et al., 2011).
153
154 In guard cells, the SAL1-PAP pathway functions in parallel to the canonical ABA signaling
155 (RCAR/PYL-OST1-PP2C) pathway to induce stomatal closure, at least in part via transcriptional
156 upregulation of CPKs which converge upon, and activate, OST1 target proteins such as the SLAC1
157 anion channel (Pornsiriwong et al., 2017). Intriguingly, PAP appears to have contrasting effects on

158 ROS in different cell types. While constitutive PAP accumulation leads to decreased ROS in
159 vascular bundles (Estavillo et al., 2011), exogenous PAP application induces ROS in guard cells
160 (Pornsiriwong et al., 2017). Constitutively accumulated PAP also rescues ABA-induced ROS burst
161 in *ost1 sal1* guard cells (Pornsiriwong et al., 2017). However, the mechanism was not investigated,
162 beyond establishing that most downstream canonical ABA-regulated processes, such as ion fluxes,
163 were activated by PAP in *ost1* mutants.
164
165 These contrasting roles for PAP as an initiator and repressor of ROS signaling in different cell types
166 raise the hypothesis tested herein that chloroplasts and their retrograde signals can function
167 differently depending on cellular context. Further, despite the parallels in chloroplast-sourced
168 retrograde ROS signaling and apoplast-sourced secondary messenger ROS signaling, there is a
169 distinct lack of knowledge how these two processes are intertwined in stress signaling. In this work
170 we explore how SAL1-PAP retrograde signaling intersects with whole-leaf ROS responses such as
171 basal plasmodesmal permeability, flg22-induced ROS responses and tolerance to ozone-derived
172 apoplastic ROS. To define how PAP, and consequently chloroplastic signals, can intersect with
173 ROS signaling, we use the guard cell as a model to study the specializations of each pathway. This
174 includes considerations of the sites of ROS accumulation, phosphorylation targets of CPKs and the
175 extent to which ABA-mediated and PAP-mediated signaling require chloroplast functionality as well
176 as retrograde signaling for stomatal closure.
177
178 **Results**
179
180 *Subcellular guard cell ROS compartmentalization is mediated by retrograde signaling for stomatal*
181 *closure*
182 Previously, we showed that ROS signaling was restored by PAP in ABA signaling mutants, but we
183 did not determine the subcellular source of ROS nor its regulation (Pornsiriwong et al., 2017).
184 Herein we examined the spatial distribution of ROS in response to exogenous PAP application

185 using H_2DCFDA which acts as a general ROS marker by reacting with H_2O_2 and other radicals
186 such as OH· (Akter et al., 2021). H_2DCFDA has been used to visualize ROS accumulation in whole
187 leaves and subcellular compartments of guard cells (Postiglione and Muday, 2023; Watkins et al.,
188 2017; Zandalinas et al., 2020).
189
190 We observed that PAP and ABA elevated ROS in multiple guard cell subcellular compartments,
191 with a notable and significant increase in chloroplasts (Fig. 1A, B). ABA treatments induced
192 chloroplastic ROS to a lower extent than PAP (Fig. 1B). The observed increase in H_2DCFDA
193 fluorescence by approximately 1.2 - 1.5-fold in response to 10 min treatment with PAP or ABA (Fig.
194 1A, B) is similar to that previously reported for H_2DCFDA fluorescence in *Arabidopsis thaliana*
195 (*Arabidopsis*) and tomato guard cells after 15 min of ABA treatment (Postiglione and Muday, 2023;
196 Watkins et al., 2017). We also visualized ROS accumulation in PAP-treated guard cells using the
197 H_2O_2-specific fluorescent dye Peroxy Orange 1 (PO1) (Dickinson et al., 2010) and found
198 comparable PAP-induced fluorescence increases in the guard cell between H_2DCFDA and PO1
199 (Fig. 1A, Fig. S1), consistent with previous observations (Postiglione and Muday, 2023; Watkins et
200 al., 2017; Zandalinas et al., 2020). Consequently, we conclude that PAP induces accumulation of
201 ROS, including H_2O_2, in guard cells.
202
203 To test whether the effect of PAP on chloroplast ROS requires ABA signaling components, we
204 investigated PAP treatment in an *ost1-2* background which is deficient in ABA signaling and
205 consequently ABA-induced stomatal closure (Mustilli et al., 2002; Pornsiriwong et al., 2017). PAP
206 still induced chloroplast ROS in *ost1-2* (Fig. 1C) while ABA did not, suggesting that PAP acts
207 independently of ABA in the induction of chloroplast ROS.
208
209 Given PAP is reported to lower, not raise, chloroplast ROS in mesophyll and bundle sheath leaf
210 tissues we investigated further the interaction between PAP and chloroplastic ROS using
211 biochemical and genetic tools. The chloroplast photosynthetic electron transport chain is a major

212 source of ROS in chloroplasts (Waszczak et al., 2018). Therefore, we attempted to attenuate
213 chloroplastic ROS production using different concentrations of the photosynthesis inhibitor 3-(3-4,-
214 dichlorophenyl)-1,1-dimethylurea (DCMU) on *Arabidopsis* epidermal peels. As expected, we
215 observed incremental reduction of the effective PSII quantum yield (Y(II)) of mesophyll tissue in
216 response to the increasing concentrations of DCMU (Fig. S2); whereas Y(II) in the guard cells was
217 below the detection threshold. We used this decrease of Y(II) in the mesophyll to infer that Y(II)
218 was similarly decreased in the chloroplasts of guard cells given the similarity of chloroplast
219 photosynthesis in both cell types (Lawson et al., 2003, 2008). Inhibition of guard cell photosynthesis
220 and chloroplastic ROS production at 10 μM DCMU decreased both ROS accumulation in guard
221 cells and guard cell chloroplasts treated with ABA or PAP (Fig. 1B). This decreased ROS correlated
222 with impaired ABA- or PAP-induced stomatal closure when co-treated with a range of DCMU
223 concentrations (Fig. 1D, S3). Intriguingly, this PAP-induced increase in ROS level driven by the
224 light reactions of photosynthesis was not associated with any changes to the low light regime; that
225 is, there was no requirement for co-treatment with high light as would be typically expected for
226 chloroplastic ROS production.
227
228 To further test if chloroplastic PSI ROS contributes to PAP-mediated stomatal closure, we utilized
229 a thylakoid ascorbate peroxidase (tAPX) over-expressor (tAPX-OE) line (Murgia et al., 2004). This
230 transgenic line has high levels of tAPX activity for catalyzing the reduction of chloroplastic H_2O_2 to
231 water. We hypothesized that increased scavenging of chloroplastic PSI ROS would prevent PAP-
232 mediated stomatal closure. Indeed, PAP-mediated stomatal closure was inhibited in tAPX-OE in
233 comparison to wild type (Fig. 1E).
234
235 As chloroplast-nuclear proximity and H_2O_2 transfer between these compartments in photosynthetic
236 tissues have been proposed as a key signaling mechanism (Exposito-Rodriguez et al., 2017), we
237 examined these processes in the context of PAP signaling in guard cells. We first verified that PAP
238 also induces an increase in ROS levels in the nucleus of guard cells by overlay of H_2DCFDA

239 fluorescence with that of the nuclear marker DAPI (Fig. S4). Given the finding that PAP can induce
240 chloroplastic ROS in *ost1*-2 (Fig. 1C), we quantified H_2DCFDA fluorescence in both chloroplasts
241 and the nucleus in parallel and found that PAP treatment increases ROS levels in the nucleus to a
242 higher degree than in the chloroplasts (Fig. 1C).
243
244 We then examined whether there was a spatial aspect to this chloroplast-nuclear ROS increase.
245 Specifically, did chloroplasts associated with the nucleus respond differently to PAP compared to
246 chloroplasts elsewhere in the cell? First, we determined whether PAP treatment altered the
247 localization of chloroplasts within a guard cell. Of the three to six chloroplasts per single guard cell,
248 one or two chloroplasts were typically associated with the junction between two guard cells, two to
249 three chloroplasts with the nucleus, and one or none in neither location (classed as 'other', Fig.
250 S5). The number of chloroplasts associated at the junction, nucleus or 'other' location was not
251 affected by PAP treatment (Fig. S5). Significantly, PAP induced ROS to a similar extent in all guard
252 cell chloroplasts regardless of location, including those associated with the nucleus (Fig. S6).
253 Collectively, the pattern of PAP-induced ROS accumulation in both chloroplasts and the nucleus of
254 guard cells is very similar to that induced by ABA (Postiglione and Muday, 2023; Watkins et al.,
255 2017). Therefore, our results indicate that like ABA, PAP induces ROS production in guard cell
256 chloroplasts, with the ROS capable of accumulating to high levels in the nucleus.
257
258 *Apoplastic ROS production by RBOHD is required for PAP-mediated signaling processes*

259 While apoplastic ROS is required for stomatal closure mediated by ABA (Rodrigues et al., 2017),
260 the role and genetic components for this process have not been identified for PAP-mediated
261 stomatal closure. We found that the double mutant *rbohDrbohF* (*rbohDF*) did not close stomata in
262 response to PAP and had the expected impaired ABA-mediated stomatal closure (June M. Kwak
263 et al., 2003) (Fig. 2A). Interestingly, we found that the single knockout *rbohF* mutant was
264 responsive to PAP but had completely impaired ABA-mediated stomatal closure (i.e., no different
265 to the control). In contrast, ABA induced stomatal closure in *rbohD*, but PAP could not. Indeed,

266 while ABA induced a significant increase in ROS of *rbohD* guard cells, PAP treatment on *rbohD* did
267 not (Fig. 2B); this was also the case for when chloroplastic ROS was measured by quantifying
268 H_2DCFDA fluorescence specifically in areas overlapping with chlorophyll fluorescence (Fig.
269 2B). This indicates that ABA induces ROS via RBOHF whereas PAP acts through RBOHD,
270 which marks an important delineation between ABA- and PAP-mediated stomatal closure.
271
272 The requirement of RBOHD for PAP-induced chloroplastic ROS (Fig. 2B) would suggest that
273 production of plastidial ROS is initiated by extracellular ROS in this signaling cascade. We then
274 tested the reverse hypothesis, that is, apoplastic ROS production requires chloroplastic ROS. We
275 utilized a modified form of H_2DCFDA, Oxyburst Green H2HFF-BSA, which is restricted to the
276 apoplast and thus acts as a general ROS marker specifically in this compartment (Miller et al.,
277 2010). PAP treatment induced an increase in apoplastic Oxyburst Green H2HFF-BSA fluorescence
278 in guard cells compared to mock treatment as expected (Fig. S7). Inhibition of chloroplast ROS
279 production led to a visible decrease in apoplastic Oxyburst Green H2HFF-BSA fluorescence in
280 guard cells co-treated with PAP and DCMU (Fig. S7). Taken together, our data suggest that the
281 effect of PAP on subcellular ROS is multifaceted, with PAP-induced ROS production in chloroplasts
282 and the apoplast influencing each other.
283
284 *PAP-induced CPKs activate RBOHD and SLAC1 thereby simultaneously impacting ROS and anion*
285 *currents in stomatal closure*
286 The induction of RBOHD activity for ROS production is thought to occur both by calcium transients
287 and protein kinase activation (Lee et al., 2020; Li et al., 2014; Zhang et al., 2018). Intracellular
288 calcium binds to the EF-hand motifs of RBOH, and calcium influx can lead to the activation of
289 several kinases such as the CPKs, which can phosphorylate RBOHD at the N terminus (Dubiella
290 et al., 2013). Considering PAP requires RBOHD to initiate stomatal closure, we investigated
291 potential CPK candidates shown to be transcriptionally up-regulated by PAP (Pornsiriwong et al.,
292 2017) as enhancers of RBOHD-mediated ROS production.

293

294 To determine whether these candidate CPKs could enhance the ROS-producing activity of
295 RBOHD, we used heterologous expression in human embryonic kidney 293T (HEK293T) cells.
296 These cells lack endogenous ROS production activity under experimental conditions employed
297 herein (Bánfi et al., 2001) and are routinely used to investigate post-translational regulation of
298 RBOH activity (Chu et al., 2023; Kaya et al., 2014). Measurement of ROS in these cells by luminol-
299 amplified chemiluminescence showed that the single transfections of CPKs alone did not differ
300 significantly to the non-transfected control, indicating that the CPKs alone could not induce ROS
301 production (Fig. S8). HEK293T cells were then co-transfected with *3FLAG-RBOHD* and
302 either *CPK-3Myc*, or *3Myc-GFP* as a negative control (Fig. 3A).
303 RBOHD protein levels were homogenous between co-transfections, indicating that any differences
304 in ROS production would be due to an additional protein partner (Fig. S9). Upon stimulation with
305 ionomycin which supplies Ca^{2+} as a co-factor of RBOH proteins, the negative control HEK293T
306 cells co-expressing *3FLAG-RBOHD* and *3Myc-GFP* exhibited only a small increase in
307 luminescence, indicating minimal ROS production. By contrast, HEK293T cells co-transfected with
308 3*FLAG-RBOHD* and one of either CPK12, CPK28, CPK32 or CPK34 showed significantly
309 enhanced RBOHD-mediated ROS production compared to the negative control (Fig. 3A).
310 CPK13 did not induce significantly different ROS production compared to the control, despite
311 CPK13 being expressed to higher levels than CPK28 or CPK32 in the HEK293T cells (Fig.
312 S9). Overall, these results demonstrate that multiple, yet specific, CPKs that are transcriptionally
313 up-regulated by PAP can activate RBOHD for PAP-mediated ROS functions.

314

315 Interestingly, the RBOHD-activating kinases include CPK32 and CPK34, which we have previously
316 identified as CPKs capable of activating SLAC1 in *Xenopus laevis* oocytes (Pornsiriwong et al.,
317 2017). This raises the question of which, amongst the repertoire of PAP-upregulated CPKs, might
318 target RBOHD and SLAC1 together or individually. We therefore tested CPK8 [another CPK
319 transcriptionally upregulated in response to PAP and known to have roles in stomatal closure (Zou

320 et al., 2015)], CPK12, CPK13 and CPK28 for SLAC1 activation using the *Xenopus* heterologous
321 expression system (Fig. 3B, S10-12). CPK12 could not activate SLAC1 in oocytes, consistent with
322 findings by Brandt et al. (2012), nor could CPK28 elicit SLAC1 anion currents. However, both CPK8
323 and CPK13 could elicit SLAC1 anion currents, albeit to varying degrees in four independent
324 experiments. Overall, different members of the PAP-induced CPKs target RBOHD and SLAC1
325 either individually or collectively (Table S1).
326
327 Different kinases phosphorylate different serine sites on SLAC1 (Brandt et al., 2015, 2012; Geiger
328 et al., 2009). Serine 120 (S120) is phosphorylated by OST1, while CPK6 phosphorylates S59
329 (Brandt et al., 2015). To define whether some of our identified CPK candidates target these
330 phosphorylation sites, S59 and S120 of SLAC1 were individually or both mutated to alanine.
331 SLAC1:S59A and SLAC1:S120A were individually co-expressed in oocytes with CPK13, CPK32
332 and CPK34 (Fig. 3C, S12). Contrary to the published literature on OST1 and CPKs phosphorylating
333 distinct sites on SLAC1, either one of the S59A or S120A mutations in SLAC1 on its own led to a
334 reduction in anion currents for CPK32 and CPK34. When we mutated both serine sites (i.e.,
335 SLAC1-S59A:S120A), this led to a further reduction in anion currents for CPK13 (Fig. S12). We
336 validated these findings *in planta* by testing whether different *Arabidopsis* SLAC1 mutants
337 responded to PAP. As expected, PAP and ABA did not close stomata of *slac1-4* lacking the SLAC1
338 protein (Fig. S13). Importantly, the *slac1-S59A/S120A* double mutant which expresses SLAC1
339 containing mutated serine sites, did not close stomata when treated with PAP (Fig. 3D).
340
341 Considering these PAP-related CPKs could activate both RBOHD and the anion channel SLAC1
342 individually, or both, thereby simultaneously impacting ROS and anion currents in stomatal closure,
343 we wanted to determine whether they could compensate for the lack of OST1, an important kinase
344 that activates SLAC1 and RBOHF (Acharya et al., 2013; Sirichandra et al., 2009). We
345 transgenically over-expressed the different CPKs in the *ost1* background and performed a water-
346 loss assay on excised individual leaves of these transgenic lines. We included CPK23, which is a

347 known activator of SLAC1 involved in the ABA signaling pathway (Geiger et al., 2010) but not
348 transcriptionally PAP-induced; expressing CPK23 in *ost1* did not alter the water-loss rate when
349 compared to the empty-vector *ost1* control (Fig. 3E). In contrast, the overexpression of PAP-
350 induced CPKs in *ost1* could reduce the water loss in comparison to empty-vector *ost1* to varying
351 degrees (Fig. 3E). This indicates that PAP-induced CPKs, in particular CPK32 and CPK34, can,
352 when expressed singularly, partially compensate for the lack of OST1 *in vivo* by modulating
353 RBOHD and/or SLAC1 activity (Table S1).
354
355 *PAP intersects with ROS signaling across diverse cell types and processes*
356 ROS, in particular H_2O_2, are critical secondary messengers in many cell types and cellular
357 processes. Therefore, we explored the extent to which PAP might intersect with ROS beyond the
358 guard cell. First, we investigated whether the characteristic ROS production induced by the
359 pathogen elicitor flg22 (Li et al., 2014; Morales et al., 2016; Torres et al., 2002) is altered in *sal1*
360 leaves as a whole, given that both flg22 and now PAP (Fig. 2A) have been shown to act via RBOHD
361 in guard cells. Flg22 induced a much more pronounced 'initial' ROS burst in *sal1* in comparison to
362 wild type (Fig. 4A), while the negative control *rbohD* did not produce any ROS.
363
364 Ozone enters leaves via stomata, and is readily converted to secondary ROS including H_2O_2, super
365 oxide and hydroxyl radical in the apoplast (Vainonen and Kangasjärvi, 2015). The whole-leaf
366 response to ozone requires functional OST1 (Vahisalu et al., 2010) and perturbation of this
367 response can result in excessive damage to vascular tissue (Vahisalu et al., 2008). Considering
368 our previous finding that constitutive PAP signaling via *sal1* restores stomatal closure in *ost1*
369 (Pornsiriwong et al., 2017), we investigated whether *ost1 sal1*-6 has restored ozone tolerance. The
370 ozone-tolerant wild type (ecotype Col-0) and ozone-sensitive *ost1* plants showed the expected
371 phenotypes, with lesions formed in the midrib of all leaves of *ost1* (Fig. S14). Interestingly, fewer
372 lesions developed on *ost1 sal1*-6; and said lesions were primarily contained to the older leaves in
373 the lower part of the rosette. In accordance with this, whole plant electrolyte measurements showed

374 that the significantly greater extent of ozone-induced ion leakage in *ost1* was decreased to wild
375 type levels in *ost1 sal1-6* (Fig. 4B).
376
377 To identify putative mechanisms enabling this rescued ozone tolerance, we performed Gene
378 Ontology (GO) enrichment analysis (Tian et al., 2020) on our previously published transcriptome
379 of *ost1 sal1-6* (Pornsiriwong et al., 2017). We found significant enrichment in differentially
380 expressed genes relating to oxidation-reduction and phosphorylation, which include ROS
381 homeostasis enzymes (e.g. ascorbate peroxidases, glutathione peroxidases) and signaling kinases
382 (e.g. MAP kinases, CPKs) respectively (Table S2). Many of these genes are established
383 components of the plant cellular response to ROS (Waszczak et al., 2018). Therefore, collectively
384 our data indicate that PAP accumulation restores ozone tolerance, and thereby ROS responses,
385 in whole leaves lacking OST1.
386
387 We finally examined the effect of constitutive PAP accumulation on another cellular process which
388 utilize ROS production and/or signaling; namely cell-to-cell permeability via plasmodesmata. The
389 aperture of plasmodesmata can be dynamically regulated by ROS in roots treated with exogenous
390 H_2O_2 (Rutschow et al., 2011), and plasmodesmata have been implicated in systemic leaf-to-leaf
391 ROS signaling (Fichman et al., 2021). The *sal1* mutant alleles *sal1*-6 and *sal1*-8 showed more open
392 plasmodesmata in comparison to wild type, as indicated by greater diffusion of green fluorescent
393 protein (GFP) from the initial particle bombardment site into neighboring cells (Fig. 4C).
394 Interestingly we identified several genes related to plasmodesmata aperture regulation that
395 were also differentially expressed in *sal1*-8 compared to wild type (Table S3). Collectively, these
396 results for stomata, flg22, ozone and plasmodesmata suggest the potential for PAP to intersect
397 with ROS signaling and homeostasis in diverse cellular processes.
398
399

400 **Discussion**

401

402 Unanswered questions in the fields of ROS and retrograde signaling revolve around functional
403 redundancy versus specificity of signals, as well as a less commonly considered quandary which
404 is the spatio-temporal intersection and neofunctionalization of the different signals in specialized
405 cells. For instance, if chloroplastic H_2O_2 itself is exported to the nucleus for signaling roles
406 (Exposito-Rodriguez et al., 2017), why do plant cells require other H_2O_2-triggered retrograde
407 signals? Furthermore, signaling roles for chloroplastic and apoplastic ROS have conventionally
408 been considered separately; thus, whether and how they intersect has remained unclear. A more
409 fundamental question is if retrograde signaling is an important cellular mechanism from an
410 evolutionary perspective, how does it intersect with other stress signaling pathways? Does this
411 differ in specialized cells, such as guard cells versus established roles in mesophyll cells or
412 vasculature bundles, as is the case for hormones and secondary messages? Collectively, our
413 results suggest the potential for PAP to intersect with ROS signaling and homeostasis in diverse
414 cellular processes.

415

416 *PAP induces ROS in multiple subcellular compartments, including chloroplasts*

417 We observed that both PAP and ABA induced ROS in chloroplasts, nuclei and the apoplast of the
418 guard cells, with similar patterns of subcellular fluorescence being observed for both the general
419 ROS marker H_2DCFDA and the more H_2O_2-specific PO1 (Fig. 1, Fig. S1). Our results are consistent
420 with recent reports of ABA inducing ROS accumulation in chloroplasts, nuclei and mitochondria of
421 *Arabidopsis* and tomato guard cells (Postiglione and Muday, 2023; Watkins et al., 2017). The
422 authors also found similar extents of ROS-responsive fluorescence changes between H_2DCFDA
423 and PO1, as well as with the genetically-encoded H_2O_2 biosensor protein roGFP2-Orp1 (Postiglione
424 and Muday, 2023).

425

426 Our observed increases in H_2DCFDA fluorescence by approximately 1.5-fold in chloroplasts and
427 nuclei of wild type guard cells after 10 min treatment with PAP or ABA, when juxtaposed against
428 the unchanged fluorescence in ABA-treated *ost1* (Fig. 1A, B) indicate that these localized ROS
429 increases are genuine effects of signaling cascades in the guard cells (Fig. 1A, B) (Postiglione and
430 Muday, 2023; Watkins et al., 2017). This suggests that increases in chloroplast and nuclear ROS
431 are utilized across different signaling cascades for stomatal regulation (Postiglione and Muday,
432 2023; Watkins et al., 2017).
433
434 The inhibition of PAP-induced stomatal closure by DCMU or tAPX over-expression (Fig. 1B, D, E,
435 S3) identifies PSI and the requirement for functioning photosynthetic electron transport chain as
436 likely origins of the chloroplastic ROS required for stomatal closure. It seems that chloroplastic PSI
437 ROS and photosynthesis *per se* play important roles in guard cell signaling, with PAP, ABA and
438 apoplastic ROS among the triggers for increases in photosynthetic-generated ROS [Figure 1 and
439 (Postiglione and Muday, 2023; Watkins et al., 2017)]. Presumably there is a synergistic interaction
440 between chloroplastic ROS and RBOH-mediated ROS for stomatal closure, such as facilitating
441 calcium release thereby promoting activation of ion channels via CPKs (Demidchik and Shabala,
442 2018; Sierla et al., 2016). Consistent with this assumption, suppression of chloroplast ROS with
443 DCMU visibly decreased PAP-induced apoplastic ROS (Fig. S7).
444
445 Of note, we also observed a concurrent increase in nuclear ROS in response to PAP (Fig. 1C),
446 which is consistent with an emerging understanding of a role for transcription in stomatal function
447 (Pornsiriwong et al., 2017; Simeoni et al., 2022). Guard cells also have a higher proportion of
448 chloroplasts associated with the nucleus (Fig. S5) compared to mesophyll cells, where direct H_2O_2
449 transfer from chloroplasts to the nucleus was reported (Exposito-Rodriguez et al., 2017); however
450 we saw no evidence for PAP altering the interactions of plastids with nuclei. While well beyond the
451 scope of this study one can speculate that chloroplast-sourced ROS oxidizing guard cell nuclear
452 proteins may alter protein interactions, trafficking, conformation and function (Couturier et al., 2013;

453 Wei et al., 2020). Mining of recent proteomics studies identifying proteins with H_2O_2-sensitive
454 cysteine residues (Huang et al., 2019; Wei et al., 2020) revealed several nuclear proteins involved
455 in stomatal regulation (Chen et al., 2021; Tõldsepp et al., 2018). This list includes CO_2
456 INSENSITIVE 1 (CIS1) which is required for elevated intracellular bicarbonate-induced activation
457 of S-type anion channel currents for CO_2-induced stomatal closure (He et al., 2018). The diversity
458 of these proteins opens new research avenues for understanding chloroplastic ROS signaling.
459
460 *How do ROS from different subcellular compartments intersect for stomatal closure?*
461 Apart from direct ROS/retrograde signaling targets, an outstanding question remains; how does
462 chloroplastic ROS intersect with apoplastic ROS? We found that PAP cannot induce ROS
463 accumulation in the chloroplasts of *rbohD* (Fig. 2B), indicating that apoplastic ROS is required for
464 chloroplastic ROS accumulation, at least for stomatal closure. This is consistent with other
465 findings, where chloroplasts are a site of ROS accumulation in guard cells in response to ozone
466 which mimics apoplastic ROS (Joo et al., 2005).
467
468 It is unclear how PAP, ABA or apoplastic ROS leads to perturbation of the photosynthetic electron
469 transport chain to generate ROS in chloroplasts, but one possible pathway is via Ca^{2+} signaling or
470 homeostasis which can influence the activity of several PSI proteins and photoprotection
471 mechanisms such as cyclic electron flow, thereby affecting photosynthetic ROS accumulation
472 (Hochmal et al., 2015; Wang et al., 2019). We previously observed Ca^{2+} influx in guard cells
473 treated with PAP (Zhao et al., 2019), although the mechanism(s) by which this occurs is
474 unknown. The HPCA1 kinase has been identified as an apoplastic ROS sensor which activates
475 plasma membrane calcium channels for influx of Ca^{2+} into guard cells for stomatal closure (Wu et
476 al., 2020). However, HPCA1 likely does not function in isolation as it acts in concert with various
477 signaling kinases such as CBL4, CIPK26 and OST1 during systemic cell-to-cell ROS and Ca^{2+}
478 signaling (Fichman et al., 2022).
479

480 Additionally, it has been proposed that chloroplast and mitochondrial ROS may be interconnected
481 through the “malate valve”, where production of excess chloroplast ROS through the photosynthetic
482 electron transport chain is partially ameliorated via export of reducing equivalents such as malate
483 to the mitochondria. Malate is then oxidized to NADH, with subsequent NADH oxidation leading to
484 ROS production in mitochondria (Zhao et al., 2018, 2020). Treating guard cells with DCMU to block
485 accumulation of chloroplast ROS resulted in no increase in H_2DCFDA fluorescence when
486 measured across the entire cell (Fig. 1B). By contrast, chloroplast H_2O_2, measured using
487 chloroplast-targeted roGFP-Orp1, continued to increase even when mitochondrial ROS
488 accumulation was chemically inhibited (Postiglione and Muday, 2023). These observations suggest
489 that chloroplast ROS precedes mitochondrial ROS in stomatal closure, in agreement with the
490 malate valve model, and could also explain why apoplastic ROS is required for both chloroplast
491 ROS (Fig. 2) and mitochondrial ROS (Postiglione and Muday, 2023).
492
493 We observed that chloroplast ROS is in turn required for PAP-induced apoplastic ROS (Fig. S7),
494 which raises the possibility of a ROS positive feedback loop between the organelles. One potential
495 mechanism is linked to the possibility of chloroplast ROS export into the cytosol and nuclei directly
496 via aquaporins (Byrt et al., 2023), or indirectly via mitochondria as described above. Regardless of
497 the mechanism(s) by which chloroplast ROS is relayed to the cytosol, there are multiple cytosolic
498 and/or nuclear-localized redox sensitive kinases such as OXI1 and MAP kinases (MPKs) which
499 can activate RBOH proteins (Jalmi and Sinha, 2015).
500
501 *CPKs transcriptionally induced by PAP integrate apoplastic ROS and ion channel regulation*
502 Interestingly, some of the PAP-induced CPKs have multiple functions in guard cells i.e., activating
503 both RBOHD and SLAC1 (Table S1). Notably, the PAP-induced CPKs activate SLAC1 through at
504 least two phosphorylation sites, S59 and S120 (Fig. 3C, S10) unlike the previously reported
505 specificity of other CPKs for S59 and OST1 for S120 (Brandt et al., 2015). The multiplicity in target
506 proteins and phosphosites of PAP-induced CPKs may translate to an additive effect for stomatal

507 regulation, since the CPKs identified to have multiple targets (i.e., CPK13, CPK32 and CPK34)
508 provided the greatest degree of complementation in preventing leaf water loss when expressed in
509 the *ost1* mutant background (Fig. 3E). The upregulation of these different CPKs that are distinct to
510 those involved in ABA signaling identifies PAP as a node that connects the chloroplast, ROS and
511 calcium signaling with ion channel activity for stomatal regulation.
512
513 Our finding that the induction of stomatal closure by PAP occurs via RBOHD but not RBOHF, while
514 ABA acts primarily via RBOHF (Fig. 2) (Kwak et al., 2003), provides a distinct delineation between
515 these two drought-induced signaling molecules and their downstream pathways. Intriguingly, plants
516 under prolonged water stress have reduced stomatal sensitivity to ABA, which is exacerbated the
517 longer the water stress is sustained (i.e. 24 hours vs 14 days) (Peng and Weyers, 1994). During
518 drought ABA accumulates rapidly (~1-3 days) in *Arabidopsis* compared to the slower buildup of
519 PAP (~4-9 days) (Estavillo et al., 2011). This temporal separation of ABA and PAP accumulation
520 may be relevant. It could lead to ABA activating particular CPKs and OST1 to produce ROS, Ca^{2+}
521 and activate SLAC1 to close stomata in the earlier stages of drought. With prolonged drought
522 stress, subsequent PAP accumulation activates the parallel CPK-RBOHD-SLAC1 pathways
523 described herein to maintain stomatal closure. Taken together, this suggests that chloroplasts, via
524 signals such as PAP, co-regulate the same proteins targeted by ABA to provide a time-gated
525 reinforcement mechanism for stomatal regulation.
526
527 *Is chloroplast signaling conserved across cell types?*
528 Our observations align with the hypothesis of cell type-specific functionalization of chloroplasts and
529 the model of the sensory plastid, which proposes specialized environmental-sensing roles for
530 chloroplasts that differ by cell type (Mackenzie and Mullineaux, 2022). PAP contributes to a
531 reduction in ROS in vascular bundles and mesophyll cells, which is consistent with PAP being a
532 chloroplast ROS-triggered signal in foliar tissue (Chan et al., 2016a) that leads to the quenching of
533 excess ROS via up-regulation of the H_2O_2 scavenger *APX2* in this tissue type (Estavillo et al.,

534 2011). In contrast, PAP induces the induction of chloroplast PSI ROS in guard cells (Fig. 1). Guard
535 cells obtain energy and carbohydrates via different routes from mesophyll chloroplasts for stomatal
536 opening regulation, even though chloroplasts from both cell types are photosynthetically competent
537 (Lawson et al., 2008, 2003; Lim et al., 2022). Guard cells also have a higher proportion of
538 chloroplasts associated with the nucleus (Fig. S5) compared to mesophyll cells, where direct H_2O_2
539 transfer from chloroplasts to the nucleus was reported (Exposito-Rodriguez et al., 2017). Given that
540 SAL1 is expressed in multiple leaf cell types but is concentrated in the vascular bundles (Estavillo
541 et al., 2011), it may be that PAP accumulates, and functions, differently in different cell types during
542 stress. We summarize these putative cell-specific differences in a proposed model (Fig. 5).
543
544 Our preliminary observations suggest that PAP-mediated chloroplast signaling can intersect with
545 ROS and Ca^{2+} across different cell types and cellular processes (Fig. 4). In some cases, the
546 mechanisms by which these pathways intersect are likely similar to that in guard cells, while in
547 others there may be differences that in part reflect the roles of PAP in different cell types. The
548 enhanced extracellular ROS production when challenged with flg22 in *sal1* (with constitutively
549 accumulated PAP) (Fig. 4A) may be explained by PAP-upregulated CPKs accentuating the
550 RBOHD-mediated ROS burst in epidermal pavement cells directly exposed to flg22 in the assay
551 medium. In contrast, a steady state of increased PAP levels with coinciding lower vascular ROS
552 (Estavillo et al., 2011) and no additional stress elicitation might explain the increased plasmodesmal
553 permeability observed (Fig. 4C) as different ROS levels can modulate plasmodesmal aperture (Cui
554 and Lee, 2016; Fichman et al., 2021).
555
556 Our results herein contribute towards resolving enigmas pertaining to cell specialization and
557 sensory plastids. PAP induces accumulation of both chloroplastic and apoplastic ROS; with both
558 subcellular sources of ROS being necessary for stomatal closure (Fig. 1–2). We establish the
559 epistatic hierarchy of signaling across the cell, with PAP-induced transcriptional up-regulation of
560 CPKs enabling activation of RBOHD for the apoplastic ROS burst, which functions in tandem with

561 the chloroplastic ROS generation and stomatal closure (Fig. 3). The PAP-induced CPKs can target
562 both RBOHD and the anion channel SLAC1, including a SLAC1 phosphosite previously considered
563 to be OST1-specific, thus enabling bypass of the ABA-OST1 pathway for stomatal closure (Fig. 3).
564 Finally, the effect of PAP extends beyond guard cells as it intersects with ROS in diverse cell types
565 and processes (Fig. 4). In conclusion we illustrate how chloroplast retrograde signals can intersect
566 with and influence multiple signaling pathways to regulate plant processes in a cell type-dependent
567 manner.
568
569 **Materials and Methods**
570
571 Extended Methods and Materials are available in *SI Appendix*.
572
573 *Plant material*
574 *Arabidopsis* wild type used in this study is Columbia-0 (Col-0). Mutants and transgenic lines are in
575 the Col-0 background except for *ost1*-2, which is in the Landsberg erecta background. Lines used
576 in this study are *sal1*-6 (SALK_020882(Estavillo et al., 2011)); *sal1*-8 (CS66977; (Estavillo et al.,
577 2011)); tAPX OE (Murgia et al., 2004); *ost1*-2 (*ost1*-2,(Mustilli et al., 2002)); *rbohD* (CS9555,
578 (Torres et al., 2002)); *rbohF* (CS9557, (Torres et al., 2002)); *rbohDF* (CS9558, (Torres et al., 2002));
579 *slac1*-4 (SALK_137265, (Vahisalu et al., 2008)); *slac1*-S59A/S120A (SLAC1 S59A/S120A; (Brandt
580 et al., 2015)), *ost1* (SALK_008068, (Yoshida et al., 2002)). Candidate CPKs were transformed in
581 the Col-0 *ost1* mutant using the agrobacterium transformation floral dip method (Clough and Bent,
582 1998) and hygromycin screen (Harrison et al., 2006), for candidates cloned in the pMDC32 binary
583 vector (Curtis and Grossniklaus, 2003) with the cauliflower mosaic virus 35S promoter replaced
584 with the guard cell promoter pGC1 (Yang et al., 2008). For stomatal aperture, flg22 ROS and water-
585 loss assays, *Arabidopsis* plants were grown on soil with 16 h light at 22 °C, except for the *rboh*
586 mutants and the respective Col-0 control, which were grown at 12 h light. For confocal microscopy

587 and ozone treatment assays, *Arabidopsis* plants were grown on soil in 12 h light. For bombardment
588 assays, *Arabidopsis* plants were grown on soil with 10 h light at 22 °C.
589
590 *Microprojectile bombardment assays*
591 Bombardment assays of cytosolic GFP endoplasmic reticulum RFP (red fluorescent protein) were
592 performed as described in Tee et al. (2022). Bombardment sites were imaged 16 hours after
593 bombardment using a confocal microscope (LSM Zeiss 800) with a 20× water dipping objective (W
594 N-Achroplan 20×/0.5). GFP was excited with a 488 nm argon laser and collected at 505-530 nm,
595 while RFP was excited with a 561 nm DPSS laser and collected at 600-640 nm.
596
597 *Flg22-induced chemiluminescence ROS assay*
598 Chemiluminescence ROS assays were performed as described in Albert et al. (2015). See
599 extended methods.
600
601 *Ozone treatment*
602 Three-week-old *Arabidopsis* plants were exposed to 50 ppb ozone for six hours from 9:00 to 15:00.
603 Plants were then transferred back into the growth chamber, with damage visually being scored and
604 photographed 24 hours post exposure. For electrolyte leakage measurements, whole rosettes were
605 collected after the end of the ozone exposure (both ozone treated and those in the control condition,
606 i.e., plants left in the growth chamber at <20 ppb ozone) and placed into 20 mL of MilliQ H_2O.
607 Samples were measured using a Mettler conductivity meter (Model FE30) to obtain ion readings
608 24 hours post the initial ozone exposure. Samples were frozen completely, defrosted, and then
609 measurements were taken again to obtain total ion content, with values plotted as a % total ion
610 lost.
611
612 *Stomatal aperture assay*

613 Stomatal aperture assays were performed as per Pornsiriwong et al. (2017). See extended
614 methods.
615
616 *Microscopy for epidermal peels*
617 Quantification of ROS in guard cells of epidermal peels was measured using 20 μM 2',7'-
618 dichlorodifluorescein diacetate (H_2DCFDA; Invitrogen) according to Pornsiriwong et al. (2017), with
619 epidermal peels treated as per Pornsiriwong et al. (2017). Fluorescence images were taken using
620 a Leica inverted confocal microscope using a 496-nm excitation line of an argon multiline laser.
621 H_2DCFDA fluorescence emission was detected at 505-525 nm, while chloroplast auto-fluorescence
622 was detected at 680-700 nm. Images were quantified using Fiji (NIH), with relative change in
623 fluorescence of ROS determined with images before and after treatment.
624
625 Visualization of intracellular and apoplastic ROS in guard cells was performed using 20 μM
626 H_2DCFDA or 100 μM peroxy orange 1 for H_2O_2 (PO1; Merck Sigma-Aldrich), and 100 μg/ml
627 Oxyburst Green H2HFF-BSA (Thermo Scientific), respectively. Markers for chloroplasts and nuclei
628 were chlorophyll fluorescence and 500 μM 4′,6-Diamidino-2-phenylindole dihydrochloride, 2-(4-
629 Amidinophenyl)-6-indolecarbamidine dihydrochloride (DAPI dihydrochloride; Merck Sigma-
630 Aldrich), respectively. Qualitative visualization experiments were performed using a Leica DM5500
631 epifluorescence microscope, with appropriate filter cubes for the respective fluorescent markers.
632
633 *HEK293T RBOHD ROS assay*
634 A prepared 96-well plate with HEK293T cells transfected with genes of interest [see extended
635 methods for cloning specifics, transfection protocol, and protein extraction and western blot
636 associated, adapted from Kimura et al. (2022)] was gently washed with 100 μL Hank's Balanced
637 Salt Solution [HBSS, with Ca^{2+} and Mg^{+}; ThermoFisher Scientific], and then 100 μL of the assay
638 buffer [29.9 mL HBSS, with Ca^{2+} and Mg^{+}, 90 μL of 0.002 g horseradish peroxidase dissolved in
639 100 μL HBSS solution, 18.8 μL of 0.4 M luminol] was added to each well. The plate was put into a

640 plate reader capable of polarization mode dispersion to measure luminescence at 37 °C. First,
641 luminescence was measured for 15 minutes for cells only in the assay buffer [measurement time 1
642 s/well, interval 1 min/well], then 50 µL of 3 µM ionomycin solution dissolved in the assay buffer was
643 dispensed in each well and measured for another 15 minutes.
644
645 *Electrophysiology*
646 SLAC1-mediated anion currents in oocytes were performed as per Pornsiriwong et al. (2017). See
647 extended methods.
648
649 *Statistical analyses*
650 Data presented as boxplots have the middle line marking the median, the box indicating the upper
651 and lower quartiles, and the whiskers showing the minimum and maximum values within 1.5×
652 interquartile range. Data were analyzed using RStudio 2021.09.01 Build 351/R version 4.0.3. See
653 extended methods for specifics.
654
655 **Acknowledgments**
656 We thank Professor Julian Schroeder for kindly providing the seeds of *slac1-S59A/S120A*. We
657 thank the Western Sydney University Confocal Bio-Imaging Facility for usage of the confocal
658 microscope. We thank Professor Wah Soon Chow (ANU) for guidance on usage of the DCMU
659 inhibitor, and Laura Bailey for assistance with the DAPI and Oxyburst Green H2FF-BSA
660 experiments. We received financial support from the ARC Laureate Fellowship (FL190100056 to
661 BJP); ANU scholarships (EET); ARC Discovery Early Career Researcher Award (DE210100466 to
662 KXC); ARC Future Fellowship (FT210100366 to ZHC); European Research Council (grant
663 agreement 725459, "INTERCELLAR") and the Biotechnology and Biological Research Council
664 (Institute Strategic Programme 'Plant Health' BBS/E/J/000PR9796) (AB and CF), Australian
665 Endeavour Award (6975_2018) and CSIRO Synthetic Biology Future Science Platform (MC), and
666 the Academy of Finland (decisions #275632, #28313, #312498 and #323917 for MW).

667

668

669 **References**

670 Acharya BR, Jeon BW, Zhang W, Assmann SM. 2013. Open Stomata 1 (OST1) is limiting in
671 abscisic acid responses of Arabidopsis guard cells. *New Phytol* **200**:1049–1063.
672 doi:10.1111/nph.12469

673 Akter S, Khan MS, Smith EN, Flashman E. 2021. Measuring ROS and redox markers in plant cells.
674 *RSC Chem Biol* **2**:1384–1401. doi:10.1039/D1CB00071C

675 Albert M, Butenko M, Aalen R, Felix G, Wildhagen M. 2015. Chemiluminescence Detection of the
676 Oxidative Burst in Plant Leaf Pieces. *Bio Protoc* **5**. doi:10.21769/BIOPROTOC.1423

677 Bánfi B, Molnár G, Maturana A, Steger K, Hegedûs B, Demaurex N, Krause KH. 2001. A Ca2+-
678 activated NADPH Oxidase in Testis, Spleen, and Lymph Nodes. *Journal of Biological*
679 *Chemistry* **276**:37594–37601. doi:10.1074/JBC.M103034200

680 Belin C, De Franco PO, Bourbousse C, Chaignepain S, Schmitter JM, Vavasseur A, Giraudat J,
681 Barbier-Brygoo H, Thomine S. 2006. Identification of Features Regulating OST1 Kinase
682 Activity and OST1 Function in Guard Cells. *Plant Physiol* **141**:1316–1327.
683 doi:10.1104/PP.106.079327

684 Brandt B, Brodsky DE, Xue S, Negi J, Iba K, Kangasjärvi J, Ghassemian M, Stephan AB, Hu H,
685 Schroeder JI. 2012. Reconstitution of abscisic acid activation of SLAC1 anion channel by
686 CPK6 and OST1 kinases and branched ABI1 PP2C phosphatase action. *Proc Natl Acad Sci U*
687 *S A* **109**:10593–10598. doi:10.1073/pnas.1116590109

688 Brandt B, Munemasa S, Wang C, Nguyen D, Yong T, Yang PG, Poretsky E, Belknap TF, Waadt R,
689 Alemán F, Schroeder JI. 2015. Calcium specificity signaling mechanisms in abscisic acid
690 signal transduction in Arabidopsis guard cells. *Elife* **4**:e03599. doi:10.7554/eLife.03599

691 Byrt CS, Zhang RY, Magrath I, Chan KX, De Rosa A, McGaughey S. 2023. Exploring aquaporin
692 functions during changes in leaf water potential. *Front Plant Sci* **14**.

693 Chan KX, Mabbitt PD, Phua SY, Mueller JW, Nisar N, Gigolashvili T, Stroeher E, Grassl J, Arlt W,
694 Estavillo GM, Jackson CJ, Pogson BJ. 2016a. Sensing and signaling of oxidative stress in
695 chloroplasts by inactivation of the SAL1 phosphoadenosine phosphatase. *Proc Natl Acad*
696 *Sci U S A* **113**:E4567–E4576.
697 doi:10.1073/PNAS.1604936113/SUPPL_FILE/PNAS.201604936SI.PDF

698 Chan KX, Phua SY, Crisp P, McQuinn R, Pogson BJ. 2016b. Learning the Languages of the
699 Chloroplast: Retrograde Signaling and Beyond. *Annu Rev Plant Biol* **67**:25–53.
700 doi:10.1146/ANNUREV-ARPLANT-043015-111854

701 Chen Q, Bai L, Wang W, Shi H, Ramón Botella J, Zhan Q, Liu K, Yang HQ, Song CP. 2021. COP1
702 promotes ABA-induced stomatal closure by modulating the abundance of ABI/HAB and
703 AHG3 phosphatases. *New Phytologist* **229**:2035–2049. doi:10.1111/NPH.17001

704 Chu J, Monte I, DeFalco TA, Köster P, Derbyshire P, Menke FLH, Zipfel C. 2023. Conservation of
705 the PBL-RBOH immune module in land plants. *Current Biology* **33**:1130-1137.e5.
706 doi:https://doi.org/10.1016/j.cub.2023.01.050

707 Clough SJ, Bent AF. 1998. Floral dip: a simplified method for Agrobacterium-mediated
708 transformation of Arabidopsis thaliana. *Plant J* **16**:735–743. doi:10.1046/J.1365-
709 313X.1998.00343.X

710 Couturier J, Chibani K, Jacquot JP, Rouhier N. 2013. Cysteine-based redox regulation and
711 signaling in plants. *Front Plant Sci* **4**:105. doi:10.3389/FPLS.2013.00105/BIBTEX

712 Crisp PA, Ganguly DR, Smith AB, Murray KD, Estavillo GM, Searle I, Ford E, Bogdanović O, Lister
713 R, Borevitz JO, Eichten SR, Pogson BJ. 2017. Rapid Recovery Gene Downregulation during
714 Excess-Light Stress and Recovery in Arabidopsis. *Plant Cell* **29**:1836–1863.
715 doi:10.1105/TPC.16.00828

716 Crisp PA, Smith AB, Ganguly DR, Murray KD, Eichten SR, Millar AA, Pogson BJ. 2018. RNA
717 Polymerase II Read-Through Promotes Expression of Neighboring Genes in SAL1-PAP-XRN
718 Retrograde Signaling. *Plant Physiol* **178**:1614–1630. doi:10.1104/PP.18.00758

719 Cui W, Lee J-Y. 2016. Arabidopsis callose synthases CalS1/8 regulate plasmodesmal permeability
720 during stress. *Nat Plants* **2**:16034. doi:10.1038/nplants.2016.34

721 Curtis MD, Grossniklaus U. 2003. A Gateway Cloning Vector Set for High-Throughput Functional
722 Analysis of Genes in Planta. *Plant Physiol* **133**:462. doi:10.1104/PP.103.027979

723 Cutler SR, Rodriguez PL, Finkelstein RR, Abrams SR. 2010. Abscisic Acid: Emergence of a Core
724 Signaling Network. *https://doi.org/101146/annurev-arplant-042809-112122* **61**:651–679.
725 doi:10.1146/ANNUREV-ARPLANT-042809-112122

726 Demidchik V, Shabala S. 2018. Mechanisms of cytosolic calcium elevation in plants: the role of
727 ion channels, calcium extrusion systems and NADPH oxidase-mediated "ROS-Ca2+ Hub."
728 *Funct Plant Biol* **45**:9–27. doi:10.1071/FP16420

729 Dickinson BC, Huynh C, Chang CJ. 2010. A Palette of Fluorescent Probes with Varying Emission
730 Colors for Imaging Hydrogen Peroxide Signaling in Living Cells. *J Am Chem Soc* **132**:5906–
731 5915. doi:10.1021/ja1014103

732 Drerup MM, Schlücking K, Hashimoto K, Manishankar P, Steinhorst L, Kuchitsu K, Kudla J. 2013.
733 The Calcineurin B-like calcium sensors CBL1 and CBL9 together with their interacting
734 protein kinase CIPK26 regulate the Arabidopsis NADPH oxidase RBOHF. *Mol Plant* **6**:559–
735 569. doi:10.1093/MP/SST009

736 Dubiella U, Seybold H, Durian G, Komander E, Lassig R, Witte CP, Schulze WX, Romeis T. 2013.
737 Calcium-dependent protein kinase/NADPH oxidase activation circuit is required for rapid
738 defense signal propagation. *Proc Natl Acad Sci U S A* **110**:8744–8749.
739 doi:10.1073/PNAS.1221294110

740 Estavillo Gonzalo M, Crisp PA, Pornsiriwong W, Wirtz M, Collinge D, Carrie C, Giraud E, Whelan J,
741 David P, Javot H, Brearley C, Hell R, Marin E, Pogson BJ. 2011. Evidence for a SAL1-PAP
742 Chloroplast Retrograde Pathway That Functions in Drought and High Light Signaling in
743 Arabidopsis. *Plant Cell* **23**:3992–4012. doi:10.1105/TPC.111.091033

744 Estavillo Gonzalo M., Crisp PA, Pornsiriwong W, Wirtz M, Collinge D, Carrie C, Giraud E, Whelan
745 J, David P, Javot H, Brearley C, Hell R, Marin E, Pogson BJ. 2011. Evidence for a SAL1-PAP
746 Chloroplast Retrograde Pathway That Functions in Drought and High Light Signaling in
747 Arabidopsis. *Plant Cell* **23**:3992–4012. doi:10.1105/TPC.111.091033

748 Exposito-Rodriguez M, Laissue PP, Yvon-Durocher G, Smirnoff N, Mullineaux PM. 2017.
749 Photosynthesis-dependent H2O2 transfer from chloroplasts to nuclei provides a high-light
750 signalling mechanism. *Nature Communications 2017 8:1* **8**:1–11. doi:10.1038/s41467-017-
751 00074-w

752 Fichman Y, Myers RJ, Grant DG, Mittler R. 2021. Plasmodesmata-localized proteins and ROS
753 orchestrate light-induced rapid systemic signaling in Arabidopsis. *Sci Signal* **14**:eabf0322.
754 doi:10.1126/scisignal.abf0322

755 Fichman Y, Zandalinas SI, Peck S, Luan S, Mittler R. 2022. HPCA1 is required for systemic reactive
756 oxygen species and calcium cell-to-cell signaling and plant acclimation to stress. *Plant Cell*
757 **34**:4453–4471. doi:10.1093/plcell/koac241

758 Gao X, Chen X, Lin W, Chen S, Lu D, Niu Y, Li L, Cheng C, McCormack M, Sheen J, Shan L, He P.
759 2013. Bifurcation of Arabidopsis NLR Immune Signaling via Ca2+-Dependent Protein
760 Kinases. *PLoS Pathog* **9**:e1003127. doi:10.1371/JOURNAL.PPAT.1003127

761 Geiger D, Scherzer S, Mumm P, Marten I, Ache P, Matschi S, Liese A, Wellmann C, Al-Rasheid
762 KAS, Grill E, Romeis T, Hedrich R. 2010. Guard cell anion channel SLAC1 is regulated by
763 CDPK protein kinases with distinct Ca2+ affinities. *Proceedings of the National Academy of*
764 *Sciences* **107**:8023 LP – 8028. doi:10.1073/pnas.0912030107

765 Geiger D, Scherzer S, Mumm P, Stange A, Marten I, Bauer H, Ache P, Matschi S, Liese A, Al-
766 Rasheid KAS, Romeis T, Hedrich R. 2009. Activity of guard cell anion channel SLAC1 is
767 controlled by drought-stress signaling kinase-phosphatase pair. *Proc Natl Acad Sci U S A*
768 **106**:21425–21430. doi:10.1073/pnas.0912021106

769 Harrison SJ, Mott EK, Parsley K, Aspinall S, Gray JC, Cottage A. 2006. A rapid and robust method
770 of identifying transformed Arabidopsis thaliana seedlings following floral dip
771 transformation. *Plant Methods* **2**:1–7. doi:10.1186/1746-4811-2-19/FIGURES/4

772 He J, Zhang RX, Peng K, Tagliavia C, Li S, Xue S, Liu A, Hu H, Zhang J, Hubbard KE, Held K, McAinsh
773 MR, Gray JE, Kudla J, Schroeder JI, Liang YK, Hetherington AM. 2018. The BIG protein
774 distinguishes the process of CO2-induced stomatal closure from the inhibition of stomatal
775 opening by CO2. *New Phytologist* **218**:232–241. doi:10.1111/NPH.14957

776 Hochmal AK, Schulze S, Trompelt K, Hippler M. 2015. Calcium-dependent regulation of
777 photosynthesis. *Biochimica et Biophysica Acta (BBA) - Bioenergetics* **1847**:993–1003.
778 doi:10.1016/J.BBABIO.2015.02.010

779 Huang J, Willems P, Wei B, Tian C, Ferreira RB, Bodra N, Martínez Gache SA, Wahni K, Liu K,
780 Vertommen D, Gevaert K, Carroll KS, Van Montagu M, Yang J, Van Breusegem F, Messens J.
781 2019. Mining for protein S-sulfenylation in Arabidopsis uncovers redox-sensitive sites. *Proc*
782 *Natl Acad Sci U S A* **116**:20256–20261.
783 doi:10.1073/PNAS.1906768116/SUPPL_FILE/PNAS.1906768116.SD03.XLSX

784 Imes D, Mumm P, Böhm J, Al-Rasheid KAS, Marten I, Geiger D, Hedrich R. 2013. Open stomata 1
785 (OST1) kinase controls R-type anion channel QUAC1 in Arabidopsis guard cells. *Plant J*
786 **74**:372–382. doi:10.1111/TPJ.12133

787 Jalmi S, Sinha A. 2015. ROS mediated MAPK signaling in abiotic and biotic stress- striking
788 similarities and differences. *Front Plant Sci* **6**.

789 Joo JH, Wang S, Chen JG, Jones AM, Fedoroff N V. 2005. Different signaling and cell death roles
790 of heterotrimeric G protein alpha and beta subunits in the Arabidopsis oxidative stress
791 response to ozone. *Plant Cell* **17**:957–970. doi:10.1105/TPC.104.029603

792 Kaya H, Nakajima R, Iwano M, Kanaoka MM, Kimura S, Takeda S, Kawarazaki T, Senzaki E,
793 Hamamura Y, Higashiyama T, Takayama S, Abe M, Kuchitsu K. 2014. Ca2+-Activated
794 Reactive Oxygen Species Production by Arabidopsis RbohH and RbohJ Is Essential for
795 Proper Pollen Tube Tip Growth. *Plant Cell* **26**:1069–1080. doi:10.1105/tpc.113.120642

796 Kimura S, Kaya H, Hashimoto K, Wrzaczek M, Kuchitsu K. 2022. Quantitative Analysis for ROS-
797 Producing Activity and Regulation of Plant NADPH Oxidases in HEK293T Cells. *Methods in*
798 *Molecular Biology* **2526**:107–122. doi:10.1007/978-1-0716-2469-2_8/FIGURES/5

799 Kwak June M., Mori IC, Pei ZM, Leonhard N, Angel Torres M, Dangl JL, Bloom RE, Bodde S, Jones
800 JDG, Schroeder JI. 2003. NADPH oxidase AtrbohD and AtrbohF genes function in ROS-
801 dependent ABA signaling in Arabidopsis. *EMBO J* **22**:2623–2633.
802 doi:10.1093/EMBOJ/CDG277

803 Kwak June M, Mori IC, Pei ZM, Leonhard N, Angel Torres M, Dangl JL, Bloom RE, Bodde S, Jones
804 JDG, Schroeder JI. 2003. NADPH oxidase AtrbohD and AtrbohF genes function in ROS-
805 dependent ABA signaling in Arabidopsis. *EMBO J* **22**:2623–2633.
806 doi:10.1093/EMBOJ/CDG277

807 Lawson T, Lefebvre S, Baker NR, Morison JIL, Raines CA. 2008. Reductions in mesophyll and
808 guard cell photosynthesis impact on the control of stomatal responses to light and CO2. *J*
809 *Exp Bot* **59**:3609. doi:10.1093/JXB/ERN211

810 Lawson T, Oxborough K, Morison JIL, Baker NR. 2003. The responses of guard and mesophyll cell
811 photosynthesis to CO2, O2, light, and water stress in a range of species are similar. *J Exp*
812 *Bot* **54**:1743–1752. doi:10.1093/JXB/ERG186

813 Lee DH, Lal NK, Lin ZJD, Ma S, Liu J, Castro B, Toruño T, Dinesh-Kumar SP, Coaker G. 2020.
814 Regulation of reactive oxygen species during plant immunity through phosphorylation and
815 ubiquitination of RBOHD. *Nat Commun* **11**. doi:10.1038/S41467-020-15601-5

816 Li L, Li M, Yu L, Zhou Z, Liang X, Liu Z, Cai G, Gao L, Zhang X, Wang Y, Chen S, Zhou JM. 2014. The
817 FLS2-Associated Kinase BIK1 Directly Phosphorylates the NADPH Oxidase RbohD to Control
818 Plant Immunity. *Cell Host Microbe* **15**:329–338. doi:10.1016/J.CHOM.2014.02.009

819 Lim SL, Flütsch S, Liu J, Distefano L, Santelia D, Lim BL. 2022. Arabidopsis guard cell chloroplasts
820 import cytosolic ATP for starch turnover and stomatal opening. *Nature Communications*
821 *2022 13:1* **13**:1–13. doi:10.1038/s41467-022-28263-2

822 Ma Y, Szostkiewicz I, Korte A, Moes D, Yang Y, Christmann A, Grill E. 2009. Regulators of PP2C
823 phosphatase activity function as abscisic acid sensors. *Science* **324**:1064–1068.
824 doi:10.1126/SCIENCE.1172408

825 Mackenzie SA, Mullineaux PM. 2022. Plant environmental sensing relies on specialized plastids. *J*
826 *Exp Bot* **73**:7155–7164. doi:10.1093/JXB/ERAC334

827 Maruta T, Noshi M, Tanouchi A, Tamoi M, Yabuta Y, Yoshimura K, Ishikawa T, Shigeoka S. 2012.
828 H2O2-triggered Retrograde Signaling from Chloroplasts to Nucleus Plays Specific Role in
829 Response to Stress. *J Biol Chem* **287**:11717. doi:10.1074/JBC.M111.292847

830 Miller GAD, Suzuki N, Ciftci-Yilmaz S, Mittler RON. 2010. Reactive oxygen species homeostasis
831 and signalling during drought and salinity stresses. *Plant Cell Environ* **33**:453–467.
832 doi:10.1111/j.1365-3040.2009.02041.x

833 Morales J, Kadota Y, Zipfel C, Molina A, Torres MA. 2016. The Arabidopsis NADPH oxidases
834 RbohD and RbohF display differential expression patterns and contributions during plant
835 immunity. *J Exp Bot* **67**:1663–1676. doi:10.1093/JXB/ERV558

836 Murgia I, Tarantino D, Vannini C, Bracale M, Carravieri S, Soave C. 2004. Arabidopsis thaliana
837 plants overexpressing thylakoidal ascorbate peroxidase show increased resistance to
838 Paraquat-induced photooxidative stress and to nitric oxide-induced cell death. *Plant J*
839 **38**:940–953. doi:10.1111/J.1365-313X.2004.02092.X

840 Mustilli AC, Merlot S, Vavasseur A, Fenzi F, Giraudat J. 2002. Arabidopsis OST1 protein kinase
841 mediates the regulation of stomatal aperture by abscisic acid and acts upstream of reactive
842 oxygen species production. *Plant Cell* **14**:3089–3099. doi:10.1105/TPC.007906

843 Park SY, Fung P, Nishimura N, Jensen DR, Fujii H, Zhao Y, Lumba S, Santiago J, Rodrigues A, Chow
844 TFF, Alfred SE, Bonetta D, Finkelstein R, Provart NJ, Desveaux D, Rodriguez PL, McCourt P,
845 Zhu JK, Schroeder JI, Volkman BF, Cutler SR. 2009. Abscisic acid inhibits type 2C protein
846 phosphatases via the PYR/PYL family of START proteins. *Science* **324**:1068–1071.
847 doi:10.1126/SCIENCE.1173041

848 Pei ZM, Murata Y, Benning G, Thomine S, Klüsener B, Allen GJ, Grill E, Schroeder JI. 2000.
849 Calcium channels activated by hydrogen peroxide mediate abscisic acid signalling in guard
850 cells. *Nature 2000 406:6797* **406**:731–734. doi:10.1038/35021067

851 Peng ZY, Weyers JDB. 1994. Stomatal sensitivity to abscisic acid following water deficit stress. *J*
852 *Exp Bot* **45**:835–845. doi:10.1093/JXB/45.6.835

853 Pornsiriwong W, Estavillo GM, Chan KX, Tee EE, Ganguly D, Crisp PA, Phua SY, Zhao C, Qiu J, Park
854 J, Yong MT, Nisar N, Yadav AK, Schwessinger B, Rathjen J, Cazzonelli CI, Wilson PB, Gilliham
855 M, Chen Z-H, Pogson BJ. 2017. A chloroplast retrograde signal, 3'phosphoadenosine 5'-
856 phosphate, acts as a secondary messenger in abscisic acid signaling in stomatal closure and
857 germination. *Elife* **6**. doi:10.7554/eLife.23361

858 Postiglione AE, Muday GK. 2023. Abscisic acid increases hydrogen peroxide in mitochondria to
859 facilitate stomatal closure. *Plant Physiol* **192**:469–487. doi:10.1093/plphys/kiac601

860 Rodrigues O, Reshetnyak G, Grondin A, Saijo Y, Leonhardt N, Maurel C, Verdoucq L. 2017.
861 Aquaporins facilitate hydrogen peroxide entry into guard cells to mediate ABA- and
862 pathogen-triggered stomatal closure. *Proc Natl Acad Sci U S A* **114**:9200–9205.
863 doi:10.1073/PNAS.1704754114/SUPPL_FILE/PNAS.1704754114.SM04.WMV

864 Rutschow HL, Baskin TI, Kramer EM. 2011. Regulation of Solute Flux through Plasmodesmata in
865 the Root Meristem. *Plant Physiol* **155**:1817–1826. doi:10.1104/PP.110.168187

866 Sato A, Sato Y, Fukao Y, Fujiwara M, Umezawa T, Shinozaki K, Hibi T, Taniguchi M, Miyake H,
867 Goto DB, Uozumi N. 2009. Threonine at position 306 of the KAT1 potassium channel is
868 essential for channel activity and is a target site for ABA-activated SnRK2/OST1/SnRK2.6
869 protein kinase. *Biochem J* **424**:439–448. doi:10.1042/BJ20091221

870 Sierla M, Waszczak C, Vahisalu T, Kangasjärvi J. 2016. Reactive Oxygen Species in the Regulation
871 of Stomatal Movements. *Plant Physiol* **171**:1569–1580. doi:10.1104/PP.16.00328

872 Simeoni F, Skirycz A, Simoni L, Castorina G, de Souza LP, Fernie AR, Alseekh S, Giavalisco P, Conti
873 L, Tonelli C, Galbiati M. 2022. The AtMYB60 transcription factor regulates stomatal opening
874 by modulating oxylipin synthesis in guard cells. *Scientific Reports 2022 12:1* **12**:1–12.
875 doi:10.1038/s41598-021-04433-y

876 Sirichandra C, Gu D, Hu H-CC, Davanture M, Lee S, Djaoui M, Valot B, Zivy M, Leung J, Merlot S,
877 Kwak JM. 2009. Phosphorylation of the Arabidopsis AtrbohF NADPH oxidase by OST1
878 protein kinase. *FEBS Lett* **583**:2982–2986. doi:10.1016/j.febslet.2009.08.033

879 Tee EE, Samwald S, Faulkner C. 2022. Quantification of Cell-to-Cell Connectivity Using Particle
880 Bombardment 263–272. doi:10.1007/978-1-0716-2132-5_17

881 Tian F, Yang D-C, Meng Y-Q, Jin J, Gao G. 2020. PlantRegMap: charting functional regulatory
882 maps in plants. *Nucleic Acids Res* **48**:D1104–D1113. doi:10.1093/nar/gkz1020

883 Tõldsepp K, Zhang J, Takahashi Y, Sindarovska Y, Hõrak H, Ceciliato PHO, Koolmeister K, Wang
884 YS, Vaahtera L, Jakobson L, Yeh CY, Park J, Brosche M, Kollist H, Schroeder JI. 2018.
885 Mitogen-activated protein kinases MPK4 and MPK12 are key components mediating CO2-
886 induced stomatal movements. *The Plant Journal* **96**:1018–1035. doi:10.1111/TPJ.14087

887 Torres MA, Dangl JL, Jones JDG. 2002. Arabidopsis gp91phox homologues Atrbohd and Atrbohf
888 are required for accumulation of reactive oxygen intermediates in the plant defense
889 response. *Proc Natl Acad Sci U S A* **99**:517–522. doi:10.1073/pnas.012452499

890 Vahisalu T, Kollist H, Wang YF, Nishimura N, Chan WY, Valerio G, Lamminmäki A, Brosché M,
891 Moldau H, Desikan R, Schroeder JI, Kangasjärvi J. 2008. SLAC1 is required for plant guard
892 cell S-type anion channel function in stomatal signalling. *Nature* **452**:487.
893 doi:10.1038/NATURE06608

894 Vahisalu T, Puzõrjova I, Brosché M, Valk E, Lepiku M, Moldau H, Pechter P, Wang YS, Lindgren O,
895 Salojärvi J, Loog M, Kangasjärvi J, Kollist H. 2010. Ozone-triggered rapid stomatal response
896 involves the production of reactive oxygen species, and is controlled by SLAC1 and OST1.
897 *The Plant Journal* **62**:442–453. doi:10.1111/J.1365-313X.2010.04159.X

898 Vainonen JP, Kangasjärvi J. 2015. Plant signalling in acute ozone exposure. *Plant Cell Environ*
899 **38**:240–252. doi:10.1111/pce.12273

900 Wang Q, Yang S, Wan S, Li X. 2019. The Significance of Calcium in Photosynthesis. *Int J Mol Sci*
901 **20**. doi:10.3390/IJMS20061353

902 Wang Y, Chen ZH, Zhang B, Hills A, Blatt MR. 2013. PYR/PYL/RCAR Abscisic Acid Receptors
903 Regulate K+ and Cl− Channels through Reactive Oxygen Species-Mediated Activation of
904 Ca2+ Channels at the Plasma Membrane of Intact Arabidopsis Guard Cells. *Plant Physiol*
905 **163**:566–577. doi:10.1104/PP.113.219758

906 Waszczak C, Carmody M, Kangasjärvi J. 2018. Reactive Oxygen Species in Plant Signaling.
907 *https://doi.org/101146/annurev-arplant-042817-040322* **69**:209–236.
908 doi:10.1146/ANNUREV-ARPLANT-042817-040322

909 Watkins JM, Chapman JM, Muday GK. 2017. Abscisic Acid-Induced Reactive Oxygen Species Are
910 Modulated by Flavonols to Control Stomata Aperture . *Plant Physiol* **175**:1807–1825.
911 doi:10.1104/pp.17.01010

912 Wei B, Willems P, Huang J, Tian C, Yang J, Messens J, Van Breusegem F. 2020. Identification of
913 Sulfenylated Cysteines in Arabidopsis thaliana Proteins Using a Disulfide-Linked Peptide
914 Reporter. *Front Plant Sci* **11**:777. doi:10.3389/FPLS.2020.00777/BIBTEX

915 Wu F, Chi Y, Jiang Z, Xu Y, Xie L, Huang F, Wan D, Ni J, Yuan F, Wu X, Zhang Y, Wang L, Ye R,
916 Byeon B, Wang W, Zhang S, Sima M, Chen S, Zhu M, Pei J, Johnson DM, Zhu S, Cao X, Pei C,
917 Zai Z, Liu Y, Liu T, Swift GB, Zhang W, Yu M, Hu Z, Siedow JN, Chen X, Pei ZM. 2020.
918 Hydrogen peroxide sensor HPCA1 is an LRR receptor kinase in Arabidopsis. *Nature 2020*
919 *578:7796* **578**:577–581. doi:10.1038/s41586-020-2032-3

920 Xiao Y, Savchenko T, Baidoo EEK, Chehab WE, Hayden DM, Tolstikov V, Corwin JA, Kliebenstein
921 DJ, Keasling JD, Dehesh K. 2012. Retrograde signaling by the plastidial metabolite MEcPP
922 regulates expression of nuclear stress-response genes. *Cell* **149**:1525–35.
923 doi:10.1016/j.cell.2012.04.038

924 Yang Y, Costa A, Leonhardt N, Siegel RS, Schroeder JI. 2008. Isolation of a strong Arabidopsis
925 guard cell promoter and its potential as a research tool. *Plant Methods* **4**:1–15.
926 doi:10.1186/1746-4811-4-6/FIGURES/6

927 Yoshida R, Hobo T, Ichimura K, Mizoguchi T, Takahashi F, Aronso J, Ecker JR, Shinozaki K. 2002.
928 ABA-Activated SnRK2 Protein Kinase is Required for Dehydration Stress Signaling in
929 Arabidopsis. *Plant Cell Physiol* **43**:1473–1483. doi:10.1093/PCP/PCF188

930 Yoshida R, Umezawa T, Mizoguchi T, Takahashi S, Takahashi F, Shinozaki K. 2006. The regulatory
931 domain of SRK2E/OST1/SnRK2.6 interacts with ABI1 and integrates abscisic acid (ABA) and
932 osmotic stress signals controlling stomatal closure in Arabidopsis. *J Biol Chem* **281**:5310–
933 5318. doi:10.1074/JBC.M509820200

934 Zandalinas SI, Fichman Y, Mittler R. 2020. Vascular Bundles Mediate Systemic Reactive Oxygen
935 Signaling during Light Stress. *Plant Cell* **32**:3425–3435. doi:10.1105/tpc.20.00453

936 Zhang M, Chiang YH, Toruño TY, Lee DH, Ma M, Liang X, Lal NK, Lemos M, Lu YJ, Ma S, Liu J, Day
937 B, Dinesh-Kumar SP, Dehesh K, Dou D, Zhou JM, Coaker G. 2018. The MAP4 Kinase SIK1
938 Ensures Robust Extracellular ROS Burst and Antibacterial Immunity in Plants. *Cell Host*
939 *Microbe* **24**:379-391.e5. doi:10.1016/J.CHOM.2018.08.007

940 Zhao C, Wang Y, Chan KX, Marchant DB, Franks PJ, Randall D, Tee EE, Chen G, Ramesh S, Phua
941 SY, Zhang B, Hills A, Dai F, Xue D, Gilliham M, Tyerman S, Nevo E, Wu F, Zhang G, Wong GK-
942 S, Leebens-Mack JH, Melkonian M, Blatt MR, Soltis PS, Soltis DE, Pogson BJ, Chen Z-H.
943 2019. Evolution of chloroplast retrograde signaling facilitates green plant adaptation to
944 land. *Proc Natl Acad Sci U S A* **116**. doi:10.1073/pnas.1812092116

945 Zhao Y, Luo L, Xu J, Xin P, Guo H, Wu J, Bai L, Wang G, Chu J, Zuo J, Yu H, Huang X, Li J. 2018.
946 Malate transported from chloroplast to mitochondrion triggers production of ROS and PCD
947 in Arabidopsis thaliana. *Cell Res* **28**:448–461. doi:10.1038/s41422-018-0024-8

948 Zhao Y, Yu H, Zhou J-M, Smith SM, Li J. 2020. Malate Circulation: Linking Chloroplast Metabolism
949 to Mitochondrial ROS. *Trends Plant Sci* **25**:446–454. doi:10.1016/j.tplants.2020.01.010

950 Zou JJ, Li XD, Ratnasekera D, Wang C, Liu WX, Song LF, Zhang WZ, Wu WH. 2015. Arabidopsis
951 CALCIUM-DEPENDENT PROTEIN KINASE8 and CATALASE3 Function in Abscisic Acid-
952 Mediated Signaling and H2O2 Homeostasis in Stomatal Guard Cells under Drought Stress.
953 *Plant Cell* **27**:1445–1460.

954

955

956

957 **Figures and Tables**

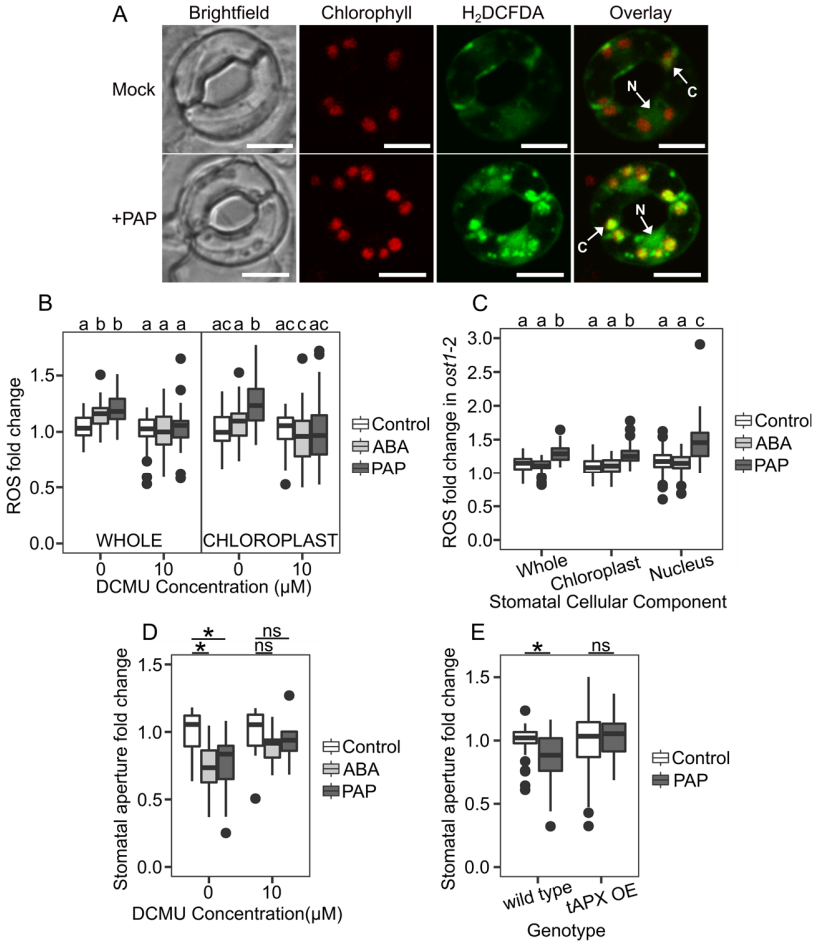

958

959 **Figure 1. Subcellular compartmentalization of ROS intersects with retrograde PAP signaling**

960 (A) Localization of ROS within guard cells treated with mock or PAP, with arrows indicating ROS
961 at chloroplasts (C) and the nucleus (N). Scale bars = 10 μM. (B) and (E) show relative change in
962 fluorescence (compared to control) in different parts of the stomata after treatment (100 μM ABA
963 or 100 μM PAP). Fluorescence is an indication of ROS levels as per the ROS dye H_2DCFDA. (B)
964 shows the relative change in fluorescence in whole guard cells or guard cell chloroplasts after
965 treatments with or without 10 μM DCMU. Each condition contains a minimum of three wild type
966 plants with n ≥ 49 stomata per treatment combination. For 'Whole', factors 'DCMU' and 'Treatment'
967 significantly impacted fluorescence with a significant interaction between the two (ANOVA; F =59.6,
968 df=1, p<0.001; F=12.0, df=2, p<0.001; F = 7.3, df=2, p<0.001). Significant differences from the

969 respective control denoted by a and b. For ‘Chloroplast’, factors ‘DCMU’ and ‘Treatment’
970 significantly impacted fluorescence, with a significant interaction between the two (ANOVA; F
971 =32.7, df=1, p<0.001; F=23.7, df=2, p<0.001; F=11.6, df=2, p<0.001). Significant differences from
972 the respective control denoted by a, b or c. For (C)**,** each treatment/subcellular component
973 combination contains a three *ost1*-2 plants with a minimum of n ≥ 40 stomata. ‘Treatment’ and ‘Part’
974 significantly impacted fluorescence (ANOVA; F=68.8, df=2, p<0.001 and F=13.4, df=2 p<0.001),
975 with a significant interaction between the two (ANOVA; F=3.2, df=4, p<0.05). Significant differences
976 denoted by a, b and c. (D) Stomatal aperture in response to 100 µM ABA or 100 µM PAP with 0 or
977 10 µM DCMU, fold change relative to DCMU control (i.e., 0 DCMU or 10 µM DCMU). Each condition
978 contains a minimum of three wild type plants with a minimum of n ≥ 27 stomata per treatment
979 combination. ‘DCMU’ and ‘Treatment’ significantly impacted closure (ANOVA; F=7.7, df=1, p<0.01;
980 F=4.2, df=2, p<0.05), with significant differences from respective control determined denoted by *,
981 p < 0.05. (E) Stomatal closure in response to 100 µM PAP in tAPX OE. Each condition contains a
982 minimum of three biological replicates with a minimum of n ≥ 41 stomata per treatment combination.
983 ‘Genotype’ significantly impacted closure (ANOVA; F= 5.4, df=1, p<0.05), with a significant
984 interaction between ‘Genotype’ and ‘Treatment’ (ANOVA; F=4.9, df=1, p<0.05). Significant
985 differences from the genotype control denoted by *, p<0.05.
986

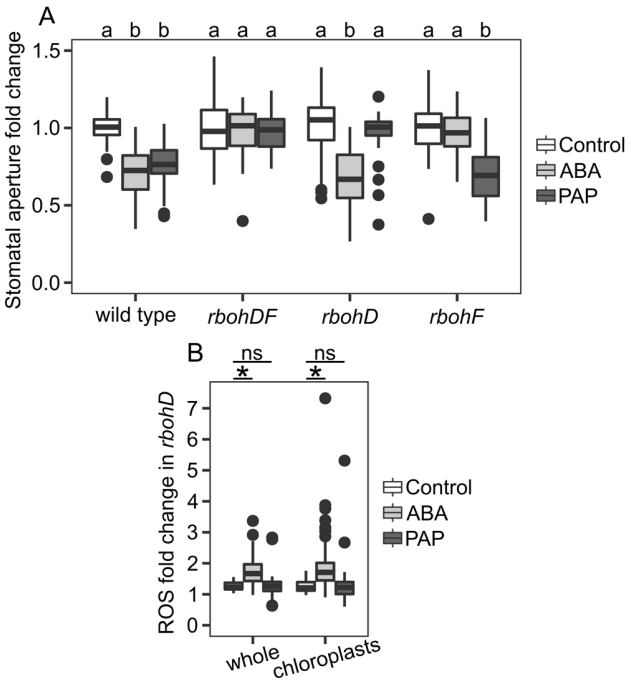

987

988 **Figure 2. *rboh* mutants are differentially perturbed in ABA and PAP-mediated stomatal**
989 **closure**

990 (A) Stomatal closure of *rboh* mutants in response to 100 μM ABA or 100 μM PAP. Each condition
991 contains a minimum of three biological replicates with a minimum of n ≥ 34 stomata per treatment
992 combination. 'Genotype' and 'Treatment' significantly impacted closure with an interaction between
993 the two (ANOVA; F=15.8, df=3, p<0.001; F=38.6, df=2, p<0.001; F=18.1, df=6, p<0.001).
994 Significant differences to the respective genotype control denoted by a or b. (B) Relative change in
995 fluorescence in whole or chloroplasts of *rbohD* guard cells as an indication of ROS levels. Each
996 condition contains a minimum of three biological replicates with a minimum of n ≥ 38 stomata per
997 treatment combination. 'Treatment' significantly impacted fluorescence in both 'whole' and
998 'chloroplasts' datasets (ANOVA; F=16.5, df=2, p<0.01; F=7.4, df=2, p<0.05), with significant
999 differences from the controls denoted by *, p<0.05.

1000

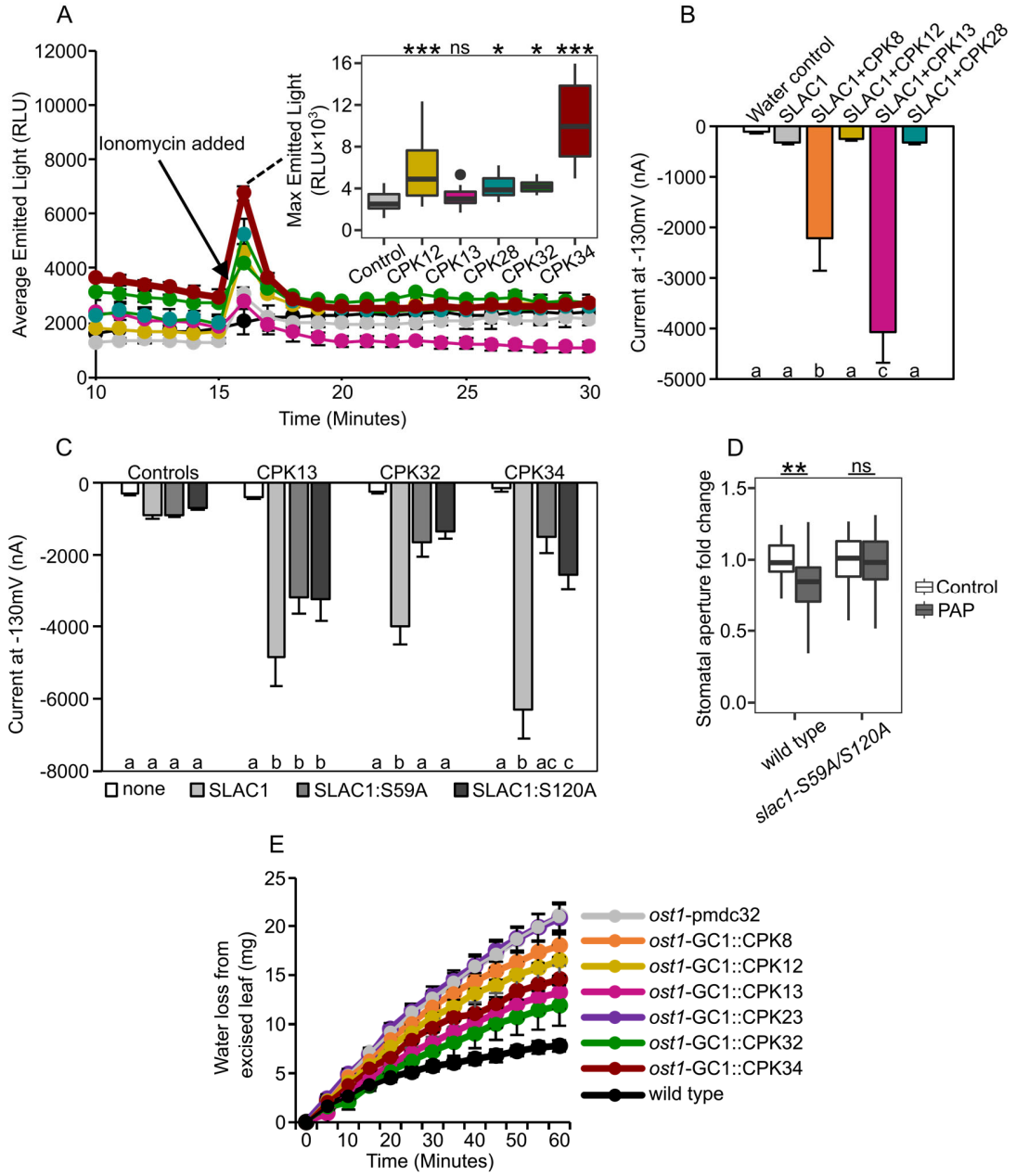

1001

1002 **Figure 3. Different PAP-induced CPKs enhance RBOHD-mediated ROS production and**

1003 **SLAC1 anion currents**

1004 (A) ROS production of HEK293T cells transiently expressing CPKs with RBOHD. After 15 min 1

1005 μM ionomycin was added to the medium. Values represent mean ± SEM for either three non-

1006 transfected replicates (shown in black), RBOHD co-transfected with GFP (control) or designated
1007 CPK. The experiment was repeated in at least four independent experiments with similar results;
1008 boxplot shows average max emitted light with data pooled from separate experiments. Control n =
1009 24, CPK12 n = 18, CPK13, 28, 32, and 34 n = 12. Factor 'Gene' expressed with RBOHD
1010 significantly impacted the max emitted light after ionomycin was added (ANOVA; F=32.3, df=5,
1011 p<0.001), with significant differences from the control denoted as * for p<0.05 or *** for p<0.0001.
1012 (B) CPK8, CPK12, CPK13 and CPK28 activation of SLAC1 anion channel in oocytes. Values are
1013 means of four to eight oocytes ± SEM. Anion channel activity shown as steady state currents
1014 activated at -130 mV, with significant differences between injected combinations (ANOVA; F=3.5,
1015 df=5, p<0.01), denoted by a, b and c. Experiment was repeated on positive candidates in two other
1016 batches of oocytes. See Fig. S7 for full trace. (C) Anion currents of mutated phosphosites in SLAC1
1017 when co-expressed with CPK13, CPK32 and CPK34 in oocytes. Values are from a minimum of five
1018 oocytes per combination ± SEM. Factors 'Type of SLAC1 expressed' and 'CPK' expressed
1019 significantly impacted the anion currents, with a significant interaction between the two (ANOVA;
1020 F=70.8, df=3, p<0.001; F=33.5, df=3, p<0.001; F=16.8, df=9, p<0.001). Significant differences with
1021 a given CPK expressed denoted by a, b and c. (D) Stomatal aperture of *slac1-S59A/S120A* mutant
1022 in response to 100 μM PAP. Each has a minimum of three biological replicates with a minimum of
1023 n ≥ 31 stomata per genotype/treatment combination. Factors 'Genotype' and 'Treatment'
1024 significantly impacted closure with a significant interaction between the two (ANOVA; F=6.3, df=1,
1025 p<0.05; F=6.4, df=1, p<0.05; F = 5.5, df=1, p<0.05). Significant differences from the genotype
1026 control denoted by **, p<0.01. (E) Water loss assay in excised leaves of *ost1* complemented with
1027 guard-cell promoter expressed CPKs. Independent transgenics lines, where n = 8, 17, 14, 9, 13, 6,
1028 14 and 11 respectively for *ost1*-pmdc32, *ost1*-GC::CPK8, *ost1*-GC::CPK12, *ost1*-GC::CPK13, *ost1*-
1029 GC::CPK23, *ost1*-GC::CPK32, *ost1*-GC::CPK34, and wild type.

1030

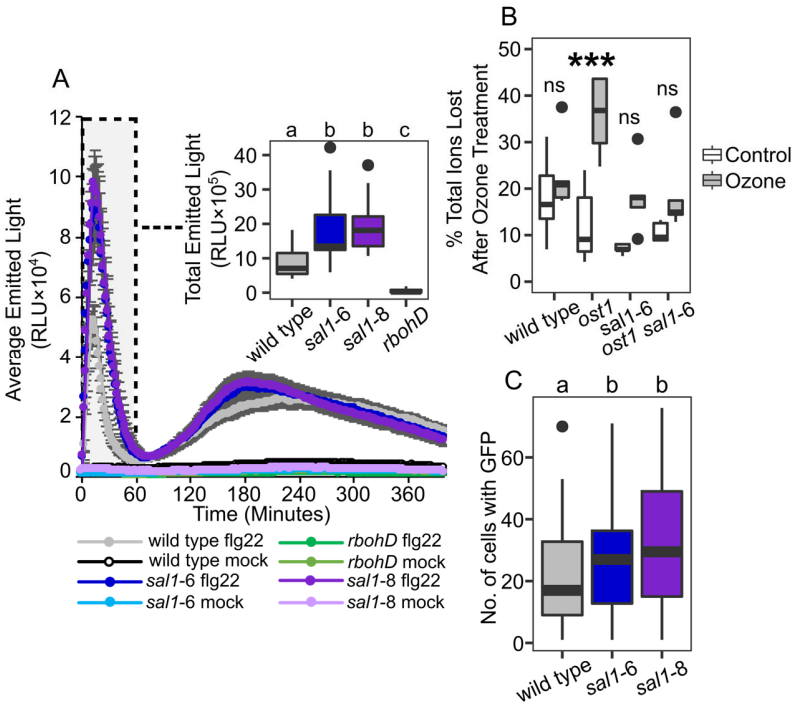

Figure 4. Altered cellular ROS processes in *sal1 mutant.*

(A) Flg22 chemiluminescence response kinetics in Arabidopsis *sal1* mutant leaf discs. Average of five-week-old plants ± SEM (eight per genotype and treatment), with data combined from two separate experiments (n=16). Boxplot shows total emitted light over 60 minutes for wild type, *sal1*-6 and *sal1*-8 and *rbohD* in response to flg22. Independent factor 'Genotype' was determined as significant (ANOVA; F=36.6, df=3, p<0.001); significant differences between genotypes denoted by a, b and c. (B) Electrolyte leakage measurements from plants harvested after six-hour exposure to ozone, 24 hours after start of ozone exposure. Values are plotted as a % total ion lost, with n = 5 per genotype and treatment. Factors 'Genotype' and 'Treatment' had a significant impact on total ion lost (ANOVA; F=4.7, df=3, p<0.01 and F=25.5, df=1, p<0.001), with significant differences between treatments within a genotype denoted by ***, p<0.001. (C) Microprojectile bombardment into leaf tissue of *sal1*-6, *sal1*-8 and wild type show *sal1* mutants have more GFP movement to neighboring cells than wild type. Number of bombardment sites counted ≥84 per genotype, three leaves × three different plants per genotype. Experiment repeated with similar significant trends found. Significance differences between genotypes indicated by a and b.

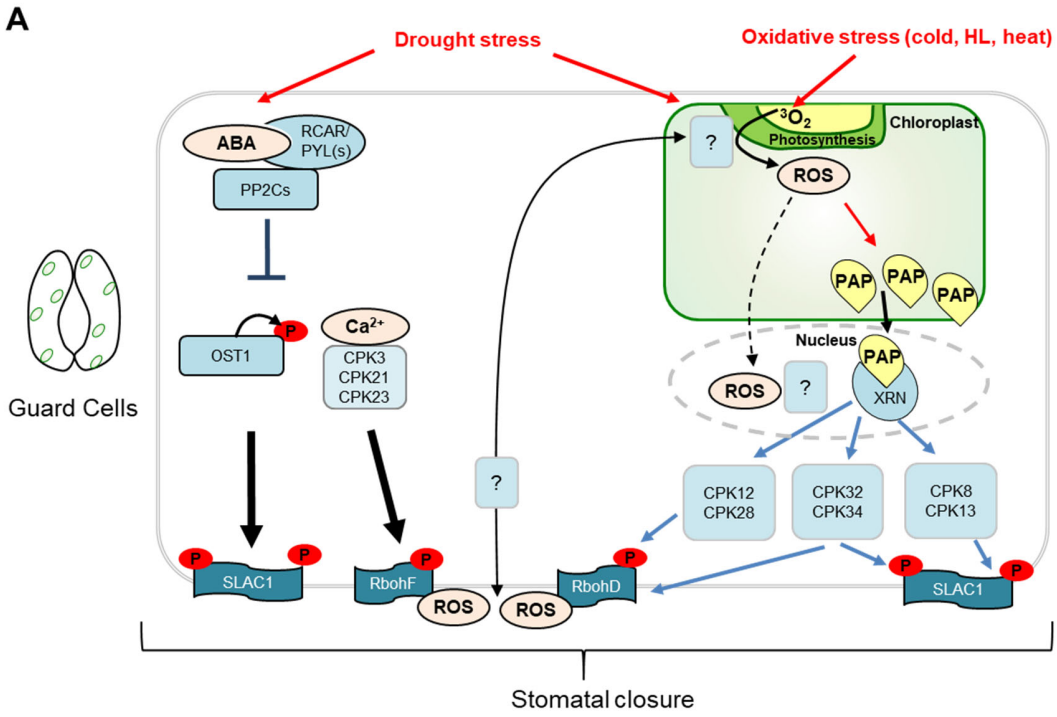
A
Drought stress
Oxidative stress (cold, HL, heat)
ABA
RCAR/
PYL(s)
PP2Cs
OST1
P
Ca2+
CPK3
CPK21
CPK23
Guard Cells
?
3O2
Photosynthesis
Chloroplast
ROS
PAP
PAP
PAP
Nucleus
PAP
ROS
?
XRN
?
CPK12
CPK28
CPK32
CPK34
CPK8
CPK13
SLAC1
RbohF
RbohD
ROS
ROS
SLAC1
Stomatal closure

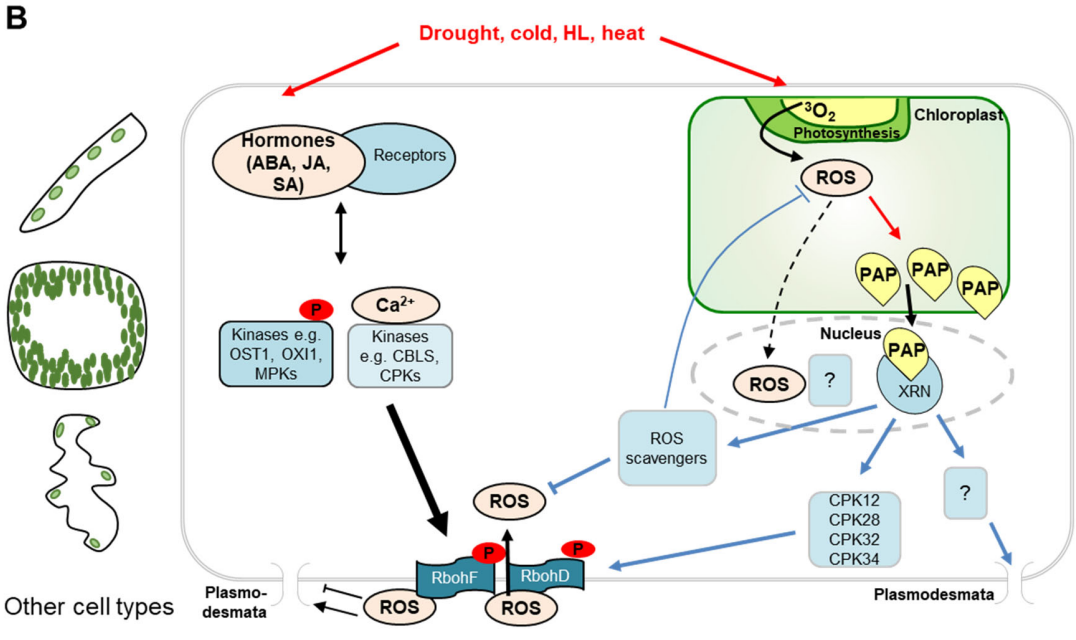
B
Drought, cold, HL, heat
Hormones
(ABA, JA,
SA)
Receptors
P
Kinases e.g.
OST1, OXI1,
MPKs
Ca2+
Kinases
e.g. CBLS,
CPKs
3O2
Photosynthesis
Chloroplast
ROS
PAP
PAP
PAP
Nucleus
PAP
ROS
?
XRN
ROS
scavengers
ROS
CPK12
CPK28
CPK32
CPK34
?
RbohF
RbohD
ROS
ROS
Other cell types
Plasmo-
desmata
Plasmodesmata

1047

1048 **Figure 5. Putative model for differential interactions between PAP and ROS in specialized**
1049 **cell types.**
1050 (A) In guard cells, PAP functions in parallel to ABA signaling to induce ROS production in
1051 chloroplasts, the nucleus, and the apoplast. Some of the CPKs transcriptionally induced by PAP
1052 can activate RBOHD for apoplastic ROS production, in contrast to ABA signaling via OST1 and
1053 other CPKs which target RBOHF. Some of the PAP-induced CPKs can activate both RBOHD and
1054 SLAC1, thus explaining the ability of PAP to function in parallel to ABA. Both chloroplast and
1055 apoplastic ROS are required for stomatal closure, and ROS production in both compartments are
1056 interdependent via unknown mechanisms. (B) In other leaf cell types such as bundle sheath,
1057 mesophyll and epidermal pavement cells, PAP has different effects on ROS accumulation and
1058 processes downstream of ROS. While PAP-induced CPKs may activate RBOHD for apoplastic
1059 ROS production and regulate plasmodesmal opening, PAP also induces expression of ROS
1060 scavengers which suppress ROS accumulation in these cell types. There is no evidence that PAP
1061 induces chloroplast or nuclear ROS in cell types other than guard cells. Other hormones and Ca^{2+}
1062 signaling can also activate RBOH-mediated apoplastic ROS production, but their intersection with
1063 PAP in these cell types remains unclear.